PLOS ONE

RESEARCH ARTICLE

A linked land-sea modeling framework to inform ridge-to-reef management in high oceanic islands

Jade M. S. Delevaux[1]*, Robert Whittier[2], Kostantinos A. Stamoulis[3,4], Leah L. Bremer[5,6], Stacy Jupiter[7], Alan M. Friedlander[1,4,8], Matthew Poti[9,10], Greg Guannel[11], Natalie Kurashima[12], Kawika B. Winter[1,13], Robert Toonen[14], Eric Conklin[15], Chad Wiggins[15], Anders Knudby[16], Whitney Goodell[4], Kimberly Burnett[5], Susan Yee[17], Hla Htun[1], Kirsten L. L. Oleson[1], Tracy Wiegner[18], Tamara Ticktin[19]

1 Department of Natural Resources and Environmental Management, University of Hawai'i, Honolulu, Hawai'i, United States of America, **2** Hawai'i Department of Health, Honolulu, Hawai'i, United States of America, **3** Department of Environment and Agriculture, Curtin University, Perth, Australia, **4** Fisheries Ecology Research Lab, University of Hawai'i, Honolulu, Hawai'i, United States of America, **5** University of Hawaii Economic Research Organization, University of Hawai'i, Honolulu, Hawai'i, United States of America, **6** University of Hawai'i Water Resources Research Center, University of Hawai'i, Honolulu, Hawai'i, United States of America, **7** Wildlife Conservation Society, Melanesia Program, Suva, Fiji, **8** National Geography Society, Washington, DC, United States of America, **9** CSS, Inc., Fairfax, Virginia, United States of America, **10** NOAA National Centers for Coastal Ocean Science, Silver Spring, Maryland, United States of America, **11** Natural Capital Project, Stanford University, Palo Alto, California, United States of America, **12** Kamehameha Schools Natural and Cultural Resources, Kailua-Kona, Hawai'i, United States of America, **13** Limahuli Garden and Preserve, National Tropical Botanical Garden, Hā'ena, Hawai'i, United States of America, **14** Hawai'i Institute of Marine Biology, University of Hawai'i, Honolulu, Hawai'i, United States of America, **15** The Nature Conservancy, Hawaii Marine Program, Honolulu, Hawai'i, United States of America, **16** Department of Geography, Environment and Geomatics, University of Ottawa, Ottawa, Ontario, Canada, **17** U.S. Environmental Protection Agency, Gulf Ecology Division, Gulf Breeze, Florida, United States of America, **18** Marine Science Department, University of Hawai'i, Hilo, Hawai'i, United States of America, **19** Department of Botany, University of Hawai'i, Honolulu, Hawai'i, United States of America

* jademd@hawaii.edu

Citation: Delevaux JMS, Whittier R, Stamoulis KA, Bremer LL, Jupiter S, Friedlander AM, et al. (2018) A linked land-sea modeling framework to inform ridge-to-reef management in high oceanic islands. PLoS ONE 13(3): e0193230. https://doi.org/10.1371/journal.pone.0193230

Editor: Chaolun Allen Chen, Academia Sinica, TAIWAN

Received: July 17, 2017

Accepted: February 7, 2018

Published: March 14, 2018

Data Availability Statement: All the groundwater and coral files are available from the data repository Scholar Space (http://hdl.handle.net/10125/48550) and figshare (https://doi.org/10.6084/m9.figshare.5877396). The marine drivers are publicly available for download on a data repository hosted by NOAA (see URL https://data.nodc.noaa.gov/cgi-bin/iso?id=gov.noaa.nodc:0155189).

Funding: Funding was provided by the National Science Foundation (NSF), Coastal Science,

Abstract

Declining natural resources have led to a cultural renaissance across the Pacific that seeks to revive customary ridge-to-reef management approaches to protect freshwater and restore abundant coral reef fisheries. Effective ridge-to-reef management requires improved understanding of land-sea linkages and decision-support tools to simultaneously evaluate the effects of terrestrial and marine drivers on coral reefs, mediated by anthropogenic activities. Although a few applications have linked the effects of land cover to coral reefs, these are too coarse in resolution to inform watershed-scale management for Pacific Islands. To address this gap, we developed a novel linked land-sea modeling framework based on local data, which coupled groundwater and coral reef models at fine spatial resolution, to determine the effects of terrestrial drivers (groundwater and nutrients), mediated by human activities (land cover/use), and marine drivers (waves, geography, and habitat) on coral reefs. We applied this framework in two 'ridge-to-reef' systems (Hā'ena and Ka'ūpūlehu) subject to different natural disturbance regimes, located in the Hawaiian Archipelago. Our results indicated that coral reefs in Ka'ūpūlehu are coral-dominated with many grazers and scrapers due to low rainfall and wave power. While coral reefs in Hā'ena are dominated by crustose

Engineering and Education for Sustainability (Grant #. 1325874). Partial funding was provided by the National Oceanic and Atmospheric Administration (NOAA) Coral Reef Conservation Program (#NA13N0S4820020) (http://coralreef.noaa.gov/) and Pacific Island Climate Science Center (#G13AC00361) (http://pi-csc.soest.hawaii.edu). CSS, Inc., provided support in the form of salary for MP under NOAA contract no. DG133C11CO0019, but did not have any additional role in the study design, data collection and analysis, decision to publish, or preparation of the manuscript. The specific role of this author is articulated in the 'author contributions' section. Coastal water quality data provided for Ka'ūpūlehu was collected by undergraduate research assistants supported by the University of Hawai'i (UH) at Hilo's Marine Science Department and the UH Mānoa's Center for Microbial Oceanography Research and Education (C-MORE, Grant #. NSF/OIA 0424599) and based upon work supported by NSF (#NSF/HRD 0833211) (the analytical analyses were conducted by the UH Hilo's Analytical Laboratory and partly supported by NSF [Grant #. NSF/EPS 0903833]). The funders had no role in study design, data collection and analysis, decision to publish, or preparation of the manuscript.

Competing interests: The authors have declared that no competing interests exist. The affiliation to CSS, Inc., does not alter our adherence to PLOS ONE policies on sharing data and materials.

coralline algae with many grazers and less scrapers due to high rainfall and wave power. In general, Ka'ūpūlehu is more vulnerable to land-based nutrients and coral bleaching than Hā'ena due to high coral cover and limited dilution and mixing from low rainfall and wave power. However, the shallow and wave sheltered back-reef areas of Hā'ena, which support high coral cover and act as nursery habitat for fishes, are also vulnerable to land-based nutrients and coral bleaching. Anthropogenic sources of nutrients located upstream from these vulnerable areas are relevant locations for nutrient mitigation, such as cesspool upgrades. In this study, we located coral reefs vulnerable to land-based nutrients and linked them to priority areas to manage sources of human-derived nutrients, thereby demonstrating how this framework can inform place-based ridge-to-reef management.

Introduction

Over the past century, climate change became a global threat to coral reefs as it directly impacts corals through bleaching, ocean acidification, and intensified storms [1–3]. At the local scale, human activities also impact coral reefs through increasing land-based source pollution and fishing pressure [3–5]. These trends have led some coral reefs to shift towards algae dominated phases, causing the decline of important resources upon which human wellbeing depends [6,7]. Thus, managing for coral reef resilience has become a priority for conservation planning [8]. Resilience is the capacity of an ecosystem to cope with its disturbance regime without shifting to an alternative state, while maintaining its functions and delivery of ecosystem service [9]. Ridge-to-reef management has been widely advocated to foster coral reef resilience, though the degree to which managing local drivers can benefit coral reefs varies among places [10,11]. The types of management actions needed to maintain coral reef resilience will differ spatially, depending on the characteristics of each ridge-to-reef system.

Natural disturbance regimes have shaped the character of coral reef ecosystems over geologic time scales by changing community structures, physical environments, and resource and space availability [12]. Coral reef disturbance regimes consist of a mixture of infrequent events, such as hurricanes, which reduce habitat complexity, and more frequent events, such as waves which dictate coral growth, and freshwater inundation that increases coral mortality [4,13–15]. The structure of coral reef communities (hereafter—coral reefs) further depends on local natural and anthropogenic drivers [16,17]. Fishing is an anthropogenic driver altering the structure of fish populations by removing key functional groups, such as herbivores [18,19], which play an important role in coral reef resilience by controlling the abundance of turf and macroalgae, and freeing space for larval recruitment [16,17,20]. Terrestrial drivers (e.g., nutrients and sediment) and marine drivers (e.g., habitat topography) shape the structure of the benthic community [21–26]. Land cover/use, such as coastal development can be a source of human-derived nutrients that promote algae growth, while agriculture can increase sedimentation and cause coral mortality [26–29]. Coral reef community structure is, therefore, a result of its natural disturbance regime and a combination of local natural and anthropogenic drivers.

Community-based movements across the Pacific seek to restore customary resource management systems that recognize the importance of land and sea connections to promote social and ecological resilience, such as the *ahupua'a* (ridge-to-reef) system in Hawai'i and the concept of *vanua* in Fiji [30–33]. High Pacific islands are ideal models to study the effects of land-sea connections on coral reefs under various natural disturbance regimes [34]. As a result of

their small size and steep elevational gradients, land and sea are tightly connected through anthropogenic and natural processes [35]. Due to their volcanic origin, island age can range from zero (actively growing) to millions of years old, and thus represent different stages of erosion [36]. The trade winds combined with rain shadows from volcanic peaks result in a gradient of rainfall, with wet windward and dry leeward exposures [37,38]. Owing to their location in the Pacific ocean, wave power impacts on all shorelines under seasonal patterns governed by distant storms [39,40]. Using traditional ridge-to-reef conceptual frameworks can help us understand these systems and support the restoration of community-based management in Pacific Islands.

To manage for coral reefs resilience, decision-makers need to understand the effects of both natural and anthropogenic drivers, from ridge-to-reef [24,41]. To assess the impacts and recovery of coral reefs subject to multiple drivers, researchers have generally relied on long-term quantitative measurements, which are rare, costly, and typically conducted at limited spatial scales [42–45]. Therefore, ecological modeling is a useful tool to foster understanding of coral reefs under co-occurring drivers and inform management at relevant spatial scales [11,46]. Although a variety of models have recently been developed to explore the influence of natural and anthropogenic drivers on coral reefs, only a few have incorporated land-sea connections and found that it changed conservation priorities [27,47–54]. However, these applications remain too coarse (1 km resolution) to support watershed-scale management for high Pacific Islands.

To address this gap, we built a novel linked land-sea modeling framework at a fine spatial scale, based on local data. We applied this framework in two *ahupua'a* (Hā'ena and Ka'ūpūlehu), with different natural disturbance regimes, located at opposite ends of the main Hawaiian Islands, to compare outcomes and inform place-based ridge-to-reef management. Although both communities have recently implemented marine reserves to actively limit fishing impacts on coral reefs in each place [55–57], we developed this framework to determine the effects of land-sea connections and identify terrestrial management actions that could promote coral reef resilience. Land-sea connections can take multiple pathways, which range from streams and storm water runoff, to groundwater discharge [15,55–57]. Though less studied, groundwater has been found in many instances to exceed surface runoff and be a primary vector for land-based nutrients to coral reefs [58–61].

Ka'ūpūlehu is located in a very dry region, lacks perennial streams, and surface runoff is uncommon. Submarine groundwater discharge (SGD) was found to be the primary vector of nutrients to coastal waters in this area [59]. Although Hā'ena is located in a wet region, where surface water discharge largely exceeds SGD, Knee et al. [62] showed that SGD nutrient flux are significantly greater than surface water, and account for over 70% of the total coastal nutrient discharge. Because there is little agriculture and SGD is the primary vector for land-based nutrients in both *ahupua'a* [60,62], we linked land and sea through nutrient enriched groundwater. We, then, modeled coral reef benthic and fish indicators, derived from ecological surveys, as a function of freshwater and nutrient flux from groundwater, and important marine drivers, including waves, local geography, and habitat [22,25,63]. By calibrating this framework separately for Hā'ena and Ka'ūpūlehu, we gained insights on the relative effects of terrestrial and marine drivers on coral reefs subject to different natural disturbance regimes and examined the following research questions: (1) Where are the highest human-derived nutrient flux in each *ahupua'a*? (2) What are the drivers differentiating these two coral reef systems? (3) How are coral reefs shaped by these drivers in each place? (4) Where land-based management actions could promote resilience of these coral reefs in a changing climate?

Methods

Site descriptions

This research focused on two *ahupua'a* at the opposite ends of the main Hawaiian Islands. Hā'ena is located on the windward side of Kaua'i Island and Ka'ūpūlehu is located on the leeward side of Hawai'i Island (Fig 1A) (further described in Table 1). Geologically older and exposed to the trade winds, Hā'ena receives high rainfall, resulting in steeply eroded cliffs, with high fluvial and groundwater inputs [64]. Geologically younger and located in the rain shadows of Mauna Loa and Mauna Kea mountains, Ka'ūpūlehu is very dry and minimally eroded, resulting in poorly developed ephemeral stream channels and large SGD [55,60]. At Hā'ena, fishing pressure was relatively lower than Ka'ūpūlehu prior to the establishment of the marine closures (Fig 1C) [65].

Overview of the linked land-sea modeling framework

Our modeling framework linked land cover/use to coral reefs through nutrient-enriched groundwater flux, using spatially-explicit groundwater and coral reef predictive models calibrated with existing empirical and remote sensing data (Fig 2). Based on climate, groundwater recharge, and recharge nutrient concentration data, groundwater flow ($m^3.yr^{-1}$) and nutrient flux ($kg.yr^{-1}$) discharging at the coast were modeled using MODFLOW and MT3D-MS at Hā'ena (15x15 m) and Ka'ūpūlehu (50x50 m). Spatially explicit nutrient flux ($kg.yr^{-1}$) from land cover/use were added to the groundwater background nutrient flux. A land-sea link was created by sub-dividing the groundwater model domain into 'flow tubes' (~200 m width) ending at pour points along the shoreline using MODPATH. To quantify the different effects of freshwater and nutrient discharge on coral reefs, we computed the total groundwater flow ($m^3.yr^{-1}$) and nutrient flux ($kg.yr^{-1}$) for each flow tube using ZONEBUDGET and diffused those values from each pour point into the coastal zone using GIS distance-based models to generate the terrestrial driver grid data (60x60 m). The SWAN wave model and bathymetry data were coupled with GIS-based models, to generate marine driver grid data (geography, habitat, and waves) (60x60 m). The coral reef predictive models were Boosted Regression Trees (BRT) calibrated on local coral reef survey data, which generated response curves representing the relationships of each individual driver to each coral reef benthic and fish indicator and predicted maps of benthic (% cover) and fish ($g.m^{-2}$) indicators (60x60 m). Once calibrated on local data, this linked land-sea framework can be used as a decision-support tool to identify priority areas for nutrient mitigation.

Coral reef indicators and field data

To measure ecological resilience, we considered the abundance of four benthic groups (% cover) and the biomass of four fish groups ($g.m^{-2}$) based on their ecological roles and cultural importance to Native Hawaiians [20,67]. The benthic indicators included calcifying organisms (CCA and scleractinian corals) and benthic algae (turf and macroalgae) (see S1 Table for more details). Resource fishes identified as important for subsistence and cultural practices by Indigenous Hawaiian communities (e.g., Acanthuridae, Scaridae, Carangidae) were modeled according to their ecological role: (1) browsers, (2) grazers, (3) scrapers, and (4) piscivores (see S1 and S2 Tables for more details) [20,68–70]. We derived percent cover of the benthic indicators and biomass of the fish indicators ($g.m^{-2}$) from reef survey data collected by the Fisheries Ecology Research Lab (FERL) at the University of Hawai'i and The Hawai'i Nature Conservancy (TNC) reef monitoring program (Fig 3). At Hā'ena, the field dataset comprised 126 survey locations randomly stratified by habitat (nearshore, back-reef, and fore-reef

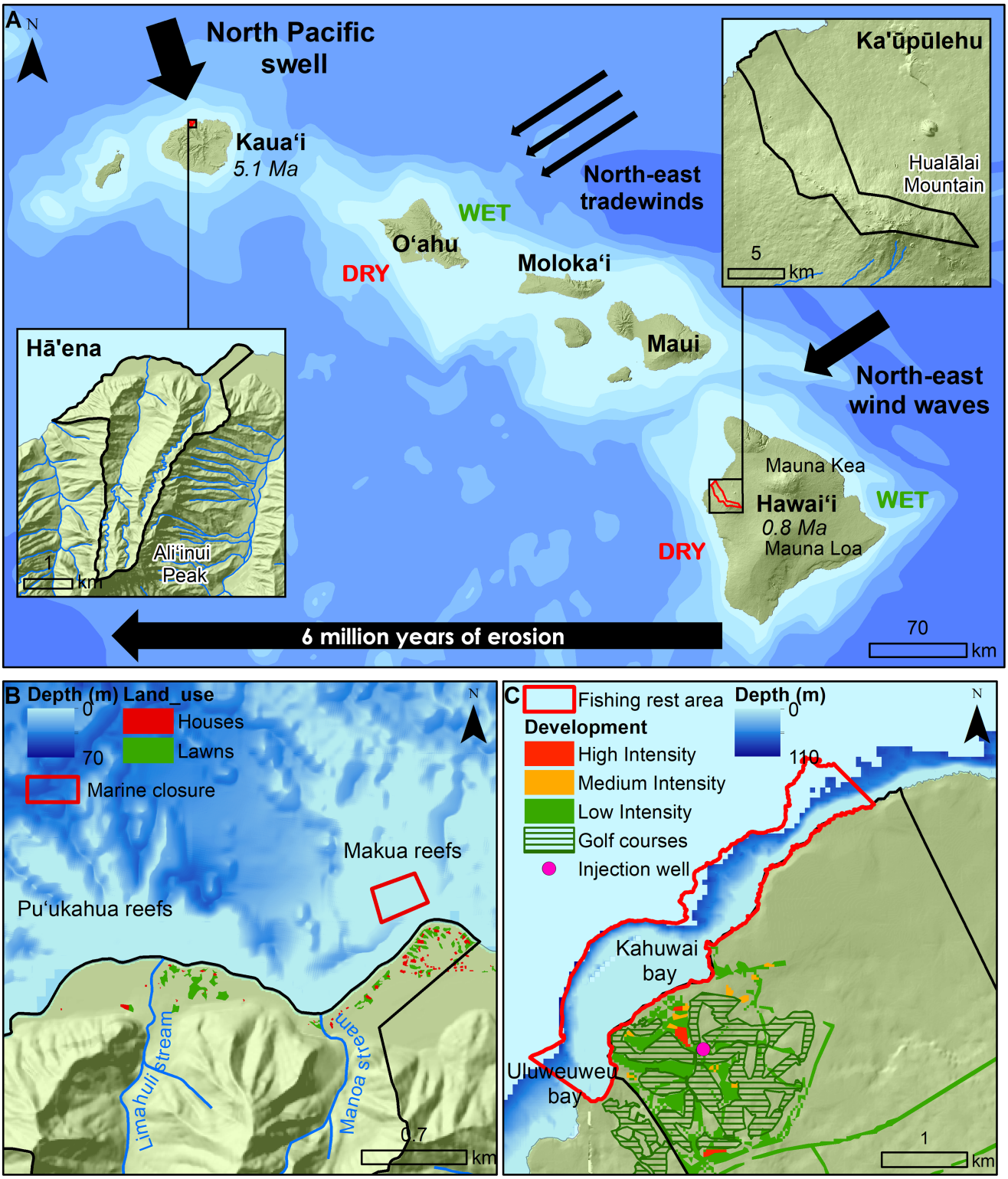

Fig 1. Study sites location. (A) Location of study sites on Kaua'i and Hawai'i along the main Hawaiian Island chain, with island age and the direction of the prevailing north-east tradewinds and ocean swell indicated. Land use/cover and marine closure/fishing rest area are shown for (B) Hā'ena and (C) Ka'ūpūlehu.

https://doi.org/10.1371/journal.pone.0193230.g001

Table 1. Study site attributes.

Attributes	Hāʻena	Kaʻūpūlehu
Island age (Ma)	5.1	0.8
Ahupuaʻa size (km^2)	7.3	104
Maximum elevation (m)	1,006 (Aliʻinui Peak)	2,518 (Hualālai Mountain)
Annual rainfall ($mm.yr^{-1}$)	High (4,040)	Low (1,350 to 260)
Perennial streams	2	0
Coastline length (km)	4	7.4
Reef area (km^2)	7.6	3.2
Dominant benthic substrate	Crustose coralline algae (CCA)	Coral
Mean total resource fish biomass ($g.m^{-2}$)	7.35	4.53
Coastal development	136 private residences	193 private residences 2 large luxury resorts 1 golf course
Management regime (year established)	Community Based Subsistence Fisheries Management Area (2016)	Community-led 10-year fishing rest period (2016)
Key land owners	State of Hawaiʻi A non-profit organization (National Tropical Botanical Garden)	Private land owner (Kamehameha Schools)

https://doi.org/10.1371/journal.pone.0193230.t001

areas) and allocated proportionately across Makua and Puʻukahua reef complex (Fig 3C), collected over two sampling periods, July 2013 and August 2014 (refer to [71] for more details). At Kaʻūpūlehu, the field dataset comprised 243 survey locations randomly stratified across two factors: management status (inside and outside the Fisheries Replenishment Area) and reef types, collected over two sampling periods, 2012 (N = 166) and 2013 (N = 78) (Fig 3D) (refer to [72] for more details).

Groundwater models

We assigned the boundary conditions of the groundwater models using MODPATH [73,74] with: (1) a flux representing the groundwater recharge at the upslope boundary; (2) no-flow condition at the lateral boundaries; and (3) the elevation of the groundwater head at the coast (layer 1) and submarine (layer 2) boundaries, based on the greater density of seawater compared to freshwater. The groundwater model domains at both sites were set to comprise the groundwater flow path from zones of recharge to coastal discharge, while spanning the entire *ahupuaʻa* boundaries and the coastal development. At Hāʻena, the groundwater model boundaries were aligned with the groundwater divides, which follow the watershed boundaries [75]. Therefore, the model domain was 6,975 ha and spanned four watersheds with perennial streams (i.e., Wainiha River [6,130 ha], Mānoa [253 ha], Limahuli [480 ha] and the Mauna Pūloʻu [112 ha] watersheds) (Fig 3A). At Kaʻūpūlehu, Engott (2011) showed that the majority of the groundwater discharging at the coastline is recharged on the upper slopes of Hualālai Mountain. Using MODPATH [74] in the reverse tracking mode, we traced the groundwater flow lines from the coastline to the upper slopes of Hualālai Mountain to delineate the Aquifer boundaries and define the zone of groundwater recharge based on the convergence of the lines. Consequently, the model domain at Kaʻūpūlehu was 33,400 ha and comprised most of the north-central and central part of the Hualālai Aquifer Sector and assumed no inter-aquifer flow between the Kīholo Aquifer and the Keauhou Aquifer, due to a rift zone bisecting the modeled area (Fig 3B). Given the different size of the model domains, we modeled Hāʻena at 15x15 m resolution and Kaʻūpūlehu at 50x50 m resolution to maintain computer efficiency.

Groundwater flow. We estimated the coastal groundwater discharge ($m^3.yr^{-1}$) using the groundwater model MODFLOW [76] and applying Eq 1 [55] at each grid cell across the

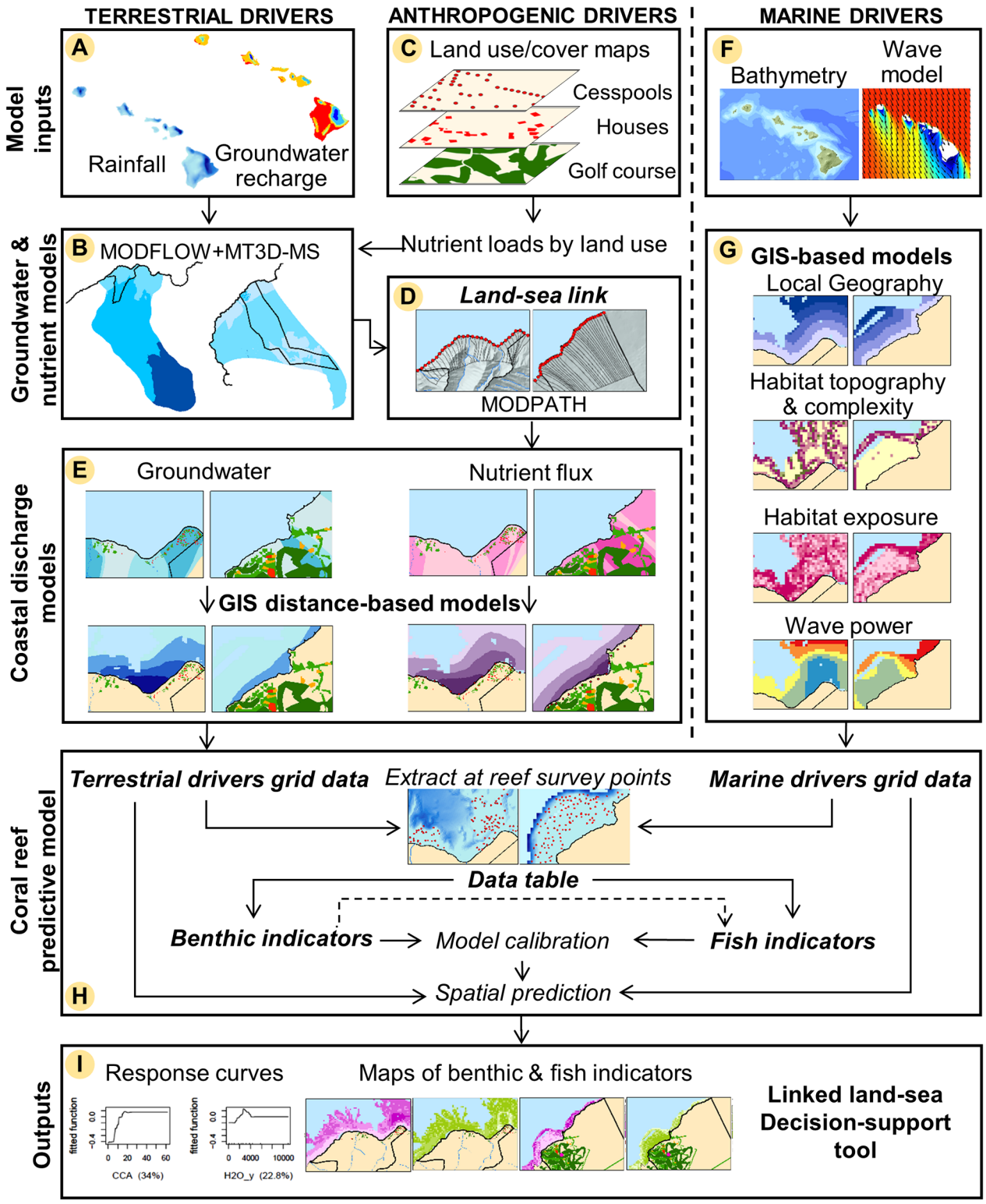

Fig 2. Linked land-sea modeling framework. Based on (A) climate, groundwater recharge, and recharge nutrient concentration data, (B) groundwater flow ($m^3.yr^{-1}$) and nutrients concentrations ($mg.L^{-1}$) were modeled using MODFLOW and MT3D-MS. (C) Nutrient flux ($kg.yr^{-1}$) from anthropogenic drivers were added to the background nutrient flux. (D) A land-sea link was created using MODPATH. (E) The coastal discharge models used the groundwater flow ($m^3.yr^{-1}$) and nutrients flux ($kg.yr^{-1}$) and GIS distance-based models to generate the terrestrial driver grid data. (F) The SWAN wave model and bathymetry data were coupled with (G) GIS-based models to generate the marine driver grid data. (H) The coral reef

predictive models were calibrated on coral reef survey data. (I) Outputs were: (1) response curves, (2) maps of benthic (% cover) and fish ($g.m^{-2}$) indicators, and (3) a linked land-sea decision-support tool. (The wave model image in panel G is reprinted from [66] under a CC BY license, with permission from Charles Fletcher, original copyright 2009. Refer to S1 File).

https://doi.org/10.1371/journal.pone.0193230.g002

model domain of both sites (Fig 2A & 2B):

$$\Delta GW = R + Inj - ET - Str - Q - Cstl \quad (1)$$

where ΔGW = change in groundwater volume (set to zero under steady state modeling), R = groundwater recharge (derived from Eq 2 for Hā'ena [77] [see below] and from the comprehensive Hawai'i Island groundwater recharge assessment at >20 m^2 resolution for Ka'ūpūlehu [55,78]), *Inj* = water injection volume into the aquifer (set to zero at Hā'ena and derived from [79] at Ka'ūpūlehu), *ET* = evapotranspiration from the aquifer (set to zero because both model domains were deeper than the maximum evapotranspiration depth [1.5 m] [78]), *Str* = groundwater discharge to streams. (At Hā'ena, we estimated at 0.26 $m^3.s^{-1}$ discharge of groundwater to Wainiha River using gauged flow data [from 2007 to present] [80] and a flow frequency distribution curve [81], then we scaled down the Wainiha River baseflow according to the relative watershed area of the other streams. At Ka'ūpūlehu, it was set to zero due to lack of perennial streams), Q = groundwater withdrawal rate (derived from [82] for both sites), *Cstl* = coastal groundwater discharge (computed as residuals).

A coarse resolution comprehensive recharge assessment was available for the Wainiha Aquifer [77]. To enhance the spatial resolution, we calculated the groundwater recharge (R) for Hā'ena by applying Eq 2 [77] at each grid cell of the model domain, which was modified to account for the leaching effluent from Onsite Sewage Disposal Systems (OSDS) into the groundwater:

$$R = P + I + OSDS - DR - AE - \Delta SS \quad (2)$$

where P = precipitation (derived from a statewide rainfall map at 250 m resolution [37]), I = irrigation (set to zero due to the lack of agriculture in the model domain), *OSDS* = leaching effluent from OSDS (refer to section 'Modeling anthropogenic drivers'), *DR* = direct runoff (assumed at 54% of rainfall [55,77]), *AE* = actual evapotranspiration (derived from a statewide evapotranspiration map at 250 m resolution [38]), and ΔSS = change in soil moisture storage (assumed to average out to zero over long term). Our calculated groundwater recharge was within 1% of the Wainiha Aquifer water budget model [77].

Groundwater nutrient concentrations. We estimated the dissolved inorganic nitrogen and phosphorus (hereafter—N and P) concentrations ($mg.L^{-1}$) using the nutrient transport model Modular Three-Dimensional Multispecies Transport Model (MT3D-MS) [83] (Fig 2B). In the absence of plant uptake at both sites, N was treated as a conservative transport species, which did not bind to soil or alter to another chemical state [84,85]. Conversely, P binds to most soils, so P concentrations reflected the leachable fraction available to the groundwater [86,87]. Given that P beneath the soil zone cannot bind with soils, we assumed no sorption for wastewater from injection wells and cesspool discharge [88]. The dispersal distance of dissolved nutrients depends on the aquifer heterogeneity, groundwater flow velocity, and molecular diffusion, and was set to 20 m according to local studies [75,88,89].

We assigned representative nutrient concentrations to the groundwater recharge based on concentrations measured in the groundwater within our model domains, thereby indirectly accounting for the biogeochemical reactions in the soil and other horizons. At Hā'ena, the background nutrient concentrations were derived from samples collected in the Wainiha Aquifer (Fig 3A) [62,90]. Given the limited groundwater samples available at Hā'ena,

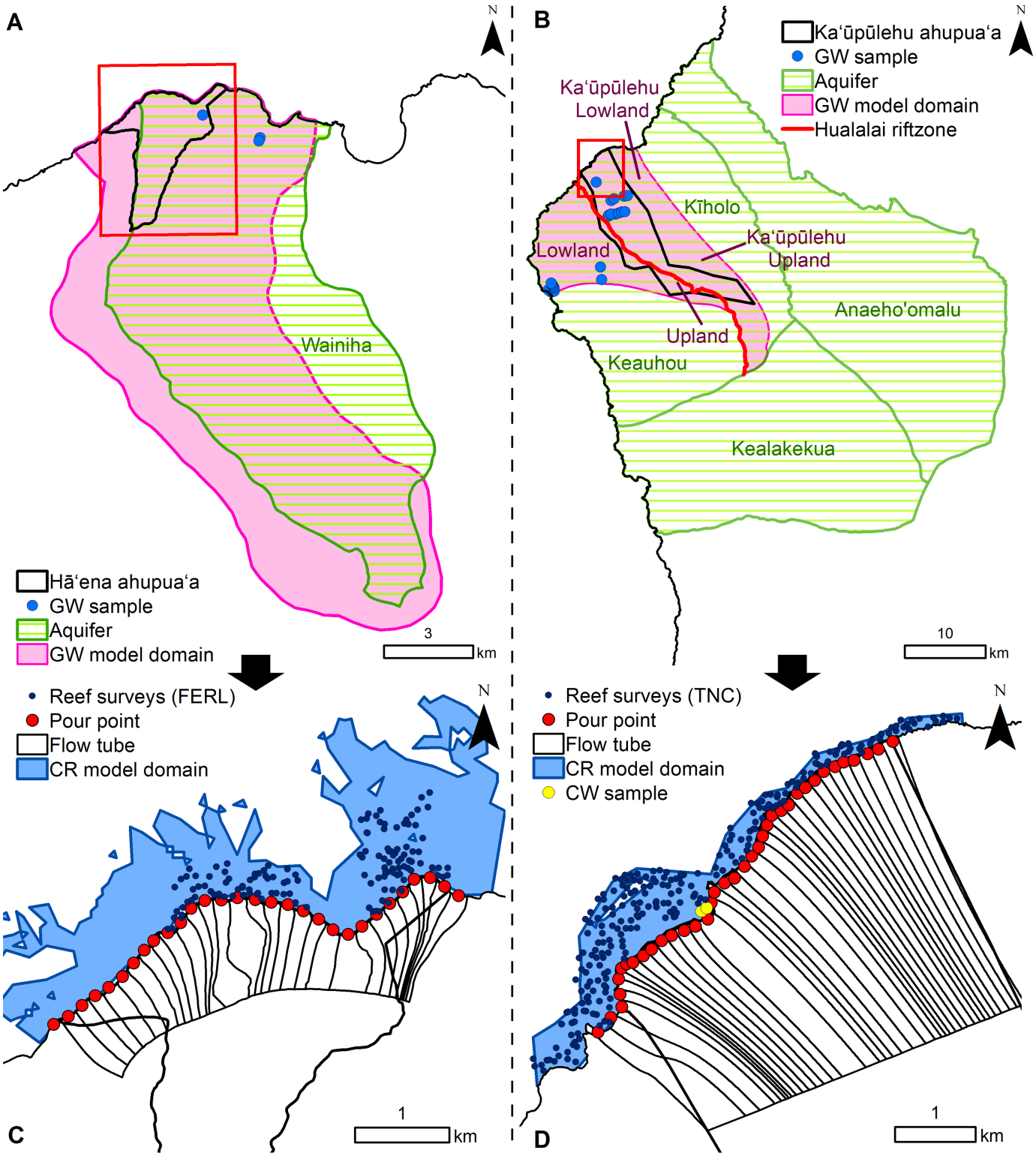

Fig 3. Model domains and land-sea link. The groundwater (GW) model domain at (A) Hā'ena (15x15 m) overlaps with the Wainiha Aquifer. The GW model domain at (B) Ka'ūpūlehu (50x50 m) was divided into 4 zones (Keauhou upland and lowland, Ka'ūpūlehu upland and lowland) and spreads across the Kīholo and Keauhou Aquifers and bisected by a rift line. In the coastal zone, the groundwater model domain was sub-divided into narrow (~200 m) flow tubes ending at pour points along the shoreline to spatially link the groundwater model outputs to SGD. Reef surveys were provided by FERL at (C) Hā'ena and TNC at (D) Ka'ūpūlehu. Based on the depth of coral reef surveys, the coral reef (CR) model domain (60x60 m) extended from the shoreline to –15 m at Hā'ena and –22 m at Ka'ūpūlehu.

https://doi.org/10.1371/journal.pone.0193230.g003

Table 2. Annual nutrient concentrations and flux of the groundwater background and land cover/use zones.

Sources	Zones	[N] ($mg.L^{-1}$)	[P] ($mg.L^{-1}$)	N flux ($kg.yr^{-1}$)	P flux ($kg.yr^{-1}$)	Source
Natural (background)	Hā'ena	0.50	0.20	$7.51.ha^{-1}$	$3.00.ha^{-1}$	[62,90]
	Ka'ūpūlehu Upland	2.70	0.20	$8.55.ha^{-1}$	$0.63.ha^{-1}$	[55,91]
	Ka'ūpūlehu Lowland	0.25	0.10	$0.65.ha^{-1}$	$0.26.ha^{-1}$	[55,91]
	Keauhou Upland	1.20	0.15	$3.11.ha^{-1}$	$0.26.ha^{-1}$	[55,91]
	Keauhou Lowland	0.25	0.1	$0.72.ha^{-1}$	$0.29.ha^{-1}$	[55,91]
Anthropogenic	Cesspool[a,b]	87	19	38	8.3	[92–95]
	Septic system[a,c]	34.2	1.2	14.9	5.2	[93,96]
	Injection well[d]	5.25	6.8	843	1300	[79]
	Lawn[e]	0.20	0.01	$4.5.ha^{-1}$	$0.2.ha^{-1}$	[97]
	Golf course[f]	7.59	0.54	$49.ha^{-1}$	$13.5.ha^{-1}$	[98]

Groundwater zones were assigned N and P recharge concentrations with the corresponding flux (i.e., concentration x annual recharge).

[a] Each land parcel assumed a residential unit with three bedrooms at an occupancy rate of 1.5 persons per bedroom generating 435 $m^3.yr^{-1}$ of wastewater [93].

[b] The nutrient loading rates were based on sampling conducted on Maui [94].

[c] The nutrient loading rates were based sampling conducted on Hawai'i Island [96].

[d] Wastewater discharge is 160,600 $m^3.yr^{-1}$ according to the State of Hawaii Injection Permit database [79].

[e] Assuming a recharge rate of 50 $m^3.ha.d^{-1}$ + background concentrations [97]

[f] Golf course fertilization rates were assumed at 879 $kg.ha^{-1}$ of N and 122 $kg.ha^{-1}$ of P, and a leaching rate of 5% for both nutrients [98].

https://doi.org/10.1371/journal.pone.0193230.t002

background nutrient concentrations were uniformly distributed across the model domain (Table 2). At Ka'ūpūlehu, the background nutrient concentrations in the Hualālai Aquifer were spatially variable, partly due to the rift zone; therefore, the model domain was divided into four zones (Ka'ūpūlehu upland and lowland, Keauhou upland and lowland) with their respective nutrients concentrations (Table 2 & Fig 3B). The nutrient concentrations for each zone were derived from Fackrell [91], who sampled 42 locations across the model domain (Fig 3B). We evaluated our modeled nutrient concentrations against these measured nutrient concentrations using linear regression (R^2 and p-value).

Human derived nutrients. To assess how coastal land cover/use influences coral reefs, we quantified N and P recharge concentrations ($mg.L^{-1}$) from coastal development in each *ahupua'a* and converted those to N and P flux ($kg.yr^{-1}$). In order to do so, we used vector maps, the houses were represented with points and the fertilized green spaces were represented by polygons delineated using aerial photos with a minimum mapping unit of 20 m^2 (Fig 2C). We then determined the wastewater treatment systems associated with each house using a statewide OSDS database [97]. These were either cesspool or septic tank systems, which both discharge effluent into the groundwater beneath the OSDS location. At Hā'ena, we estimated a total of 136 houses (99 cesspools; 37 septic systems) and 6 ha of lawn in the model domain [93]. At Ka'ūpūlehu, we estimated 193 houses with 45 ha of lawn, two resorts disposing of their wastewater after secondary treatment through an injection well, and a golf course (190 ha) [79]. The coastal nutrient flux from lawns and golf courses were based on assumed irrigation and fertilization rates [97,99]. To reflect the best management practices of the Ka'ūpūlehu community, we used lower fertilization rates on the golf course compared to urbanized areas, like West Maui [100]. We assigned N and P flux to each land cover/use derived from local data where possible, and from literature values, when local data were not available (*see* Table 2 for more details). We used the Groundwater Modeling System (GMS) interface [101] to compute the nutrient loads from the vector-based land cover maps (e.g. shapefiles) and add these fluxes to the groundwater water flow and background nutrient

flux. Within each grid cell, GMS multiplied the number of houses and area of fertilized green space with their respective nutrient flux and added these fluxes to the background water flow and nutrient flux stored in the underlying raster gridded maps (e.g., 15x15 m at Hāʻena and 50x50 m at Kaʻūpūlehu) [101].

Linking land and sea models

To link the groundwater and coral reef models and represent the non-point source nature of SGD (Fig 2D), we sub-divided the groundwater model domains into narrow flow tubes (~200 m width) ending in pour points at the shoreline using MODPATH (Fig 3C & 3D) [73,74,102]. The flow tube boundaries were established along groundwater flow path lines and assumed very little exchange of groundwater and dissolved nutrients between them. MODPATH relies on the MODFLOW groundwater flow solution to model particle movement along the simulated track to an endpoint [73,74]. Virtual particles were placed at the pour points along the shoreline and the reverse tracking option was used to delineate groundwater flow paths from the coast to the zones of recharge, through the model domain. The width of the flow tubes captured the spatial distribution of groundwater flow rates and nutrient sources from anthropogenic sources (i.e., land cover/use). The groundwater flow rates varied along coastline features, such as embayments where groundwater flow lines converged, and coastal protrusions where groundwater flow lines dispersed. The smallest land cover type was houses, aggregated into small communities, which formed the smallest spatial unit for nutrient sources. The upland extent of flow tubes was determined by a groundwater elevation contour to be consistent with groundwater flow through aquifers. The length of the flow tubes was based on the boundaries of coastal development. Because coastal development at Hāʻena was concentrated along the coastal zone, the flow tubes reached 1,000 m inland (Fig 1B). At Kaʻūpūlehu, the coastal development extended further inland so the length of the flow tubes was 3,500 m (Fig 1C). At the shoreline, the flow tube boundary corresponded to the groundwater model submarine boundary.

Because freshwater (decreases salinity) and nutrients (promote algae growth) affect coral reefs differently [103], we converted the background nutrient concentrations ($mg.L^{-1}$) into nutrient flux ($kg.yr^{-1}$) (i.e., concentration x annual recharge), using the modeled groundwater recharge ($m^3.yr^{-1}$). This allowed us to model freshwater and nutrients as separate variables and thus quantify the independent effects of freshwater and nutrient discharge on the coral reef indicators. The groundwater discharge and nutrient flux from the grid cells were then computed for each flow tube using the groundwater utility model, ZONEBUDGET [104]. This consisted of adding the water flow and nutrient fluxes from the multiple grid cell values within the boundaries of each flow tube to the groundwater flow ($m^3.yr^{-1}$) and nutrient flux ($kg.yr^{-1}$) entering the flow tubes from upslope, and discharging those in bulk at each corresponding pour point.

Modeling terrestrial drivers

We generated terrestrial drivers' grid maps (60x60 m) by diffusing the modeled groundwater discharge ($m^3.yr^{-1}$) and nutrient flux ($kg.yr^{-1}$) from each pour point into the coastal zone using ArcGIS (Fig 2E). First, we created a cost-path surface ($\boldsymbol{c}$) to quantify the least accumulative cost-distance (impedance) of moving planimetrically through each cell from each pour point, using a composite of three marine drivers known to affect diffusion (depth [m], distance from shore [m], and wave power [$kW.m^{-1}$]–see 'Modeling marine divers' for more details) [26,105]. Then, the spread of groundwater and nutrient values into coastal waters from each pour point was modeled using a decay function (*see* Eq 3), which assigned a portion of the remaining

quantity from the previous cell in all adjacent cells, based on the cost-path surface until a maximum distance of 1 km from the shoreline was reached [49,60,106–108]:

$$W_i = L_p \times e^{-c^2/D_c} \quad (3)$$

where W = Grid cell value for diffused groundwater ($m^3.yr^{-1}$) and nutrients flux ($kg.yr^{-1}$), L_p = Groundwater ($m^3.yr^{-1}$) and nutrients ($kg.yr^{-1}$) flux at each pour point (obtained from computing the groundwater and nutrient flux by flow tube), c = cost-path surface (unitless), D_c = cost-path surface threshold distance from the shore for each decayed groundwater metrics (equivalent to 1,000 m from the shoreline). This approach to modeling SGD is diffusive, and thus, allows for wrap around coastal features, but did not account for nearshore advection that acts to push the SGD in specific directions [49]. We used these diffusive models to derive conservative estimates of SGD plumes, since the nearshore circulation patterns were unknown for our study sites.

We assumed that the nutrient chemistry of the SGD was similar to that of the groundwater. Biogeochemical reactions that could occur, but were not considered in this study are those associated with denitrification and anammox (anaerobic ammonium oxidation). Given that the biogeochemical conversion of N and P to other species requires reducing conditions, the high dissolved oxygen content (dominantly >80%) in the aquifers around the main Hawaiian Islands results in stable oxidized forms of dissolved N and P, which are the dominant species [84,88,91,109]. Thus there is a possibility that we over- and under-estimated the amount of N and P, respectively, particularly at Kaʻūpūlehu, where wastewater is disposed of through injection wells [88,109]. Due to the very limited coastal water quality data in our model domains (S3 Table), these modeled terrestrial drivers could only be partially ground-truthed at Kaʻūpūlehu using linear regression (R^2 and p-value) (Fig 3D). These SGD models were meant to capture general spatial patterns, which could be refined with future SGD measurements.

Modeling marine drivers

The marine drivers grid maps (60x60 m) were derived from remote sensing and wave model data available for both sites using GIS-based tools (Fig 2F & 2G) [110]. These were identified as important drivers of coral reef benthic and fish communities based on existing literature and local community input (Table 3 & S4 Table). The wave disturbance driver was represented by mean wave power at each site ($kW.m^{-1}$) and derived from a 500 m resolution SWAN hindcast model that spanned 10 years (2000–2009) [111]. Depth and distance from shore were used to account for variation arising from spatial location. Depth was derived from a synthesis of multibeam sonar and LiDAR bathymetry at 5 m resolution, and distance from shore was derived from the statewide coastline map [112,113]. Three types of habitat drivers, representing direct and indirect effects of seafloor topography on benthic and fish communities were also derived from this bathymetry data [113]: (1) habitat topography, (2) habitat complexity, and (3) habitat exposure. Habitat topography metrics, represented by Bathymetric Position Index (BPI) and slope described the position of the reef relative to the surrounding area. These metrics were computed for two neighborhood sizes (60 and 240 m radii) to capture habitat topography at different spatial scales [114,115]. Habitat complexity metrics, represented by rugosity, planar curvature, and profile curvature were computed to describe fine-scale topographic structure. Habitat exposure metrics were used to characterize the direct and indirect effects of water flow due to fine-scale seafloor topography and directionality. These metrics were derived by computing seafloor aspect, the steepest downslope direction of the seafloor measured in degrees. We calculated the circular mean and standard deviation of aspect and

Table 3. Description of marine drivers.

Indicator[a]	Driver	Description	Unit
Wave	Power[b]	Mean wave power derived from a 10 year (2000–2009) SWAN hindcast wave model.	$kW.m^{-1}$
Geography	Depth[c]	Mean seafloor depth	m
	Distance to shore[d]	Euclidean distance to the shoreline	m
Habitat topography	BPI[c]	Relative topographic position of a point based its elevation and the mean elevation within a neighborhood (m)	m
	Slope[c]	Maximum rate of change in seafloor depth between each grid cell and its neighbors	Degrees
Habitat complexity	Planar curvature[c]	Seafloor curvature perpendicular to the direction of the maximum slope (mean). Value indicates whether flow will converge or diverge over a point.	$Radians.m^{-1}$
	Profile curvature[c]	Seafloor curvature in the direction of the maximum slope (mean). Value indicates whether flow will accelerate or decelerate over the curve.	$Radians.m^{-1}$
	Rugosity[c]	Measure of small-scale variations of amplitude in the height of a surface (mean). Value range from 1 (flat) to infinity.	Unitless
Habitat exposure	Aspect[c]	Downslope direction of maximum rate of change in seafloor depth between each grid cell and its neighbors (sine circular mean, cosine circular mean, circular standard deviation)	Degrees

Refer to S5 Table for more details on processing methods.

[a] The marine drivers were generated at 60 m resolution

[b] SWAN hindcast wave model at 500 m native resolution [113]

[c] Bathymetry synthesis at 5 m native resolution [113]

[d] Coastline [112]

https://doi.org/10.1371/journal.pone.0193230.t003

converted the circular mean into measures of northness and eastness by calculating the cosine and sine, respectively.

Identifying the drivers differentiating coral reefs

To identify the drivers differentiating the coral reefs between both sites, we used a distance based redundancy analysis (dbRDA) in PRIMER PERMANOVA+ software [116]. The dbRDA routine performed an ordination of the coral reef indicators as a function of the drivers [116,117]. A Euclidean distance similarity measure was used to construct a resemblance matrix of the transformed and normalized benthic and fish indicators. Square root and fourth root transformations were applied to the benthic and fish variables, respectively, to improve normality [63,118]. Environmental drivers were normalized, with highly correlated ($r > 0.7$) drivers removed from the models. A fitted variation >70% was considered a good fit to the model [116].

Coral reef modeling

We used BRT to build the coral reef models (Fig 2H) [119]. Tree-based models are effective at modeling nonlinearities, discontinuities (threshold effects), and interactions between variables, which is well suited for the analysis of complex ecological data [120–122]. BRT models can accommodate many types of response variables, including presence/absence, count, diversity, and abundance data [123]. Since the coral reef indicators were all continuous variables, the response variables were modeled using a Gaussian (normal) distribution, and appropriate data transformations (square root for benthic indicators and fourth root for fish biomass) were applied to improve the normality of the response variable distributions. We calibrated the BRT models on coral reef data to determine the most influential drivers (among the simultaneously tested predictors) and estimate the underlying relationship between the modeled indicators and the key drivers using response curves [123,124]. The values of the terrestrial and marine drivers' grid maps were sampled using bilinear interpolation at the location of

each reef survey (start of the transect) in ArcGIS. This approach takes a weighted average of the 4 nearest cell values, thereby accounting for the relative position of the reef surveys on the predictor grids and their different native spatial scales. The values of the coral reef indicators and interpolated terrestrial and marine drivers at these locations were combined in a single data table to calibrate the BRT models.

Each indicator was modeled independently as a function of the terrestrial and marine drivers at each site. First, we calibrated each benthic indicator model as a function of the terrestrial and marine drivers. Then, we calibrated each fish indicator model as a function of the terrestrial and marine drivers and included the empirical abundance of benthic groups as additional predictors in the models for the fish groups. The calibration process used an internal ten-fold cross-validation to maximize the model fit and determine the optimal combinations of four parameters: (1) learning rate (lr); (2) tree complexity (tc); (3) bag fraction (bag); and (4) the maximum number of trees (*see* [123] for more details). We used the percent deviance explained (PDE) and internal ten-fold cross validation PDE (CV PDE) as performance measures of the model optimum. The optimal models explained the most variation in the response variables (i.e., greatest CV PDE) and were selected as the best and final models. The model calibration was conducted in R software using the gbm package [123,125,126]. Spatial autocorrelation of the response variable was tested using Moran's I Index for both the raw values and the ecological model residuals [127].

Coral reef predictive mapping

The coral reef predictive maps were generated at 60x60 m to account for the dimensions of the reef survey methods (i.e., 25–50 m transects) and the positional accuracy of global positioning system used to navigate to them in the field [71,72]. Using the calibrated BRT models, we predicted and mapped the distribution of each coral reef indicator on a cell-by-cell basis using the values of the terrestrial and marine drivers at each cell across the coral reef model domains. The boundaries of the coral reef model domains comprised the lateral boundaries of the *ahupua'a* to capture the spatial extent of this management unit and the offshore boundary corresponded to the maximum surveyed depth (i.e., 15 m at Hā'ena and 22 m at Ka'ūpūlehu) (Fig 3C & 3D). This spatial predictive modeling method is static in nature, so we did not account for exchange between grid-cells, such as fish movement. First, we spatially predicted each benthic indicator as a function of their key drivers. Then, we spatially predicted the fish indicators as a function of their key drivers, including the predicted distribution of the benthic indicators. The predicted values of the benthic and fish grid maps were sampled using bilinear interpolation at the location of each reef survey (start of the transect) in ArcGIS, thereby accounting for the relative position of the reef surveys on the predicted grids. The values of the interpolated predictions and surveyed coral reef indicators at these locations were compared with a linear regression (R^2 and p-value). Then, we overlaid the predicted maps with the survey points values for each indicator using the same color ramp scale for the legend to enable visual comparison. The spatial predictions were performed in the R software using the dismo and raster packages [126,128,129].

Identifying priority areas for management

Once calibrated for each site, we used this framework to identify priority areas on land where management actions that reduce or limit additional nutrient inputs can promote coral reef resilience in the face of climate change. We considered a suite of criteria derived from the drivers, coral reef models, and coral reef indicators specific to each site. Based on the assumption that corals in shallow areas are more vulnerable to bleaching from increases in sea surface

temperatures [10], we focused on shallow depths at both sites (<5 m). We further considered areas with above-average (based on individual site means) coral, macroalgae or CCA, and turf algae cover, as well as high nutrient inputs and low wave mixing (based on the high and low tercile, respectively), assuming these criteria would also contribute to vulnerability to phase shifts resulting from climate induced bleaching [10,16,17,26]. Because P was not shown to be a driver of the benthic community at Hā'ena, we did not consider it here. Likewise, we did not consider wave power for Ka'ūpūlehu. For Hā'ena, we classified areas with percent cover of coral > 11.4%, macroalgae > 9.4%, and turf algae >50.0%, and areas subject to N >1,322.7 kg.yr^{-1} and wave power <19,860 $kW.m^{-1}$. At Ka'ūpūlehu, we classified areas with percent cover of coral > 18.4%, CCA > 4.1%, and turf algae >44.4%, and areas exposed to N >2,940.8 $kg.yr^{-1}$ and P >325.2 $kg.yr^{-1}$. Using raster calculations in ArcGIS, we identified coral reef areas where these criteria overlapped and were, therefore, most susceptible to future coral bleaching and nutrient impacts. By matching these coral reef areas with corresponding flow tubes with high nutrients derived from anthropogenic activities, we located priority areas on land where nutrient inputs should be limited or reduced.

Results

Groundwater models

The groundwater model results showed differences in recharge rates and nutrient concentrations between both sites. Groundwater recharge was much higher at Hā'ena (ranging from 0.11 to 4.97 $m.yr^{-1}$) compared to Ka'ūpūlehu (ranging from 0.04 to 0.69 m.yr-1) (Figs 4A & 5A). The background N concentrations were higher at Ka'ūpūlehu (0.25–2.70 $mg.L^{-1}$), compared to Hā'ena (0.5–0.85 $mg.L^{-1}$) (Figs 4B & 5B). While the background P concentrations were similar for Hā'ena (0.09–0.20 $mg.L^{-1}$) and Ka'ūpūlehu (0.10–0.20 $mg.L^{-1}$) (Figs 4D & 5D). The key sources of human-derived nutrients were wastewater from houses on cesspools at Hā'ena (Fig 4C & 4E) and the golf course and wastewater from the injection well at Ka'ūpūlehu (Fig 5C & 5E). The comparison of measured and modeled nutrient concentrations at Ka'ūpūlehu, indicated that the N model performed better compared to the P model (Fig 5B & 5D, S1 Fig). Data was insufficient to allow for a similar comparison at Hā'ena.

Terrestrial and marine coral reef drivers

According to the dbRDA (Fig 6), Hā'ena and Ka'ūpūlehu coral reefs were well separated in ordination space based on terrestrial (freshwater, N, and P) and marine (wave, distance from shore, and depth) drivers (presented in Figs 4, 5 & 7). The first axis accounted for 57.8% of the fitted variation (corresponding to 34.1% of the total variation) and the second axis accounted for 29% of the fitted variation (equivalent to 17.1% of the total variation). The first axis was primarily correlated with wave power, thereby separating the coral reefs exposed to high wave power at Hā'ena ($\bar{X} = 21,697 \pm 4,119$), from the coral reefs sheltered from wave power at Ka'ūpūlehu ($\bar{X} = 2,756 \pm 186$) (Fig 7A & 7B). The second axis was positively correlated with distance from shore and negatively correlated with depth, thereby separating the wider and shallower eroded island shelf of Hā'ena (distance to shore $\bar{X} = 594.5 \pm 422.8$ and depth $\bar{X} = -7.7 \pm 6$) from the narrow and steep island shelf of Ka'ūpūlehu (distance to shore $\bar{X} = 269.5 \pm 187.1$ and depth $\bar{X} = -8 \pm 4.7$) (Fig 7C & 7D). While not identified as primary marine drivers differentiating the sites, habitat topography metrics indicated that the reef slope was steeper at Ka'ūpūlehu ($slope_{60}$ $\bar{X} = 3.4 \pm 2.4$) compared to Hā'ena ($slope_{60}$ $\bar{X} = 2.8 \pm 1.8$) (Fig 7E & 7F), while habitat complexity was higher at Hā'ena (planar curvature $\bar{X} = 18.1 \pm 9.3$) compared to Ka'ūpūlehu (planar curvature $\bar{X} = 13.8 \pm 9.9$) (Fig 7G & 7H).

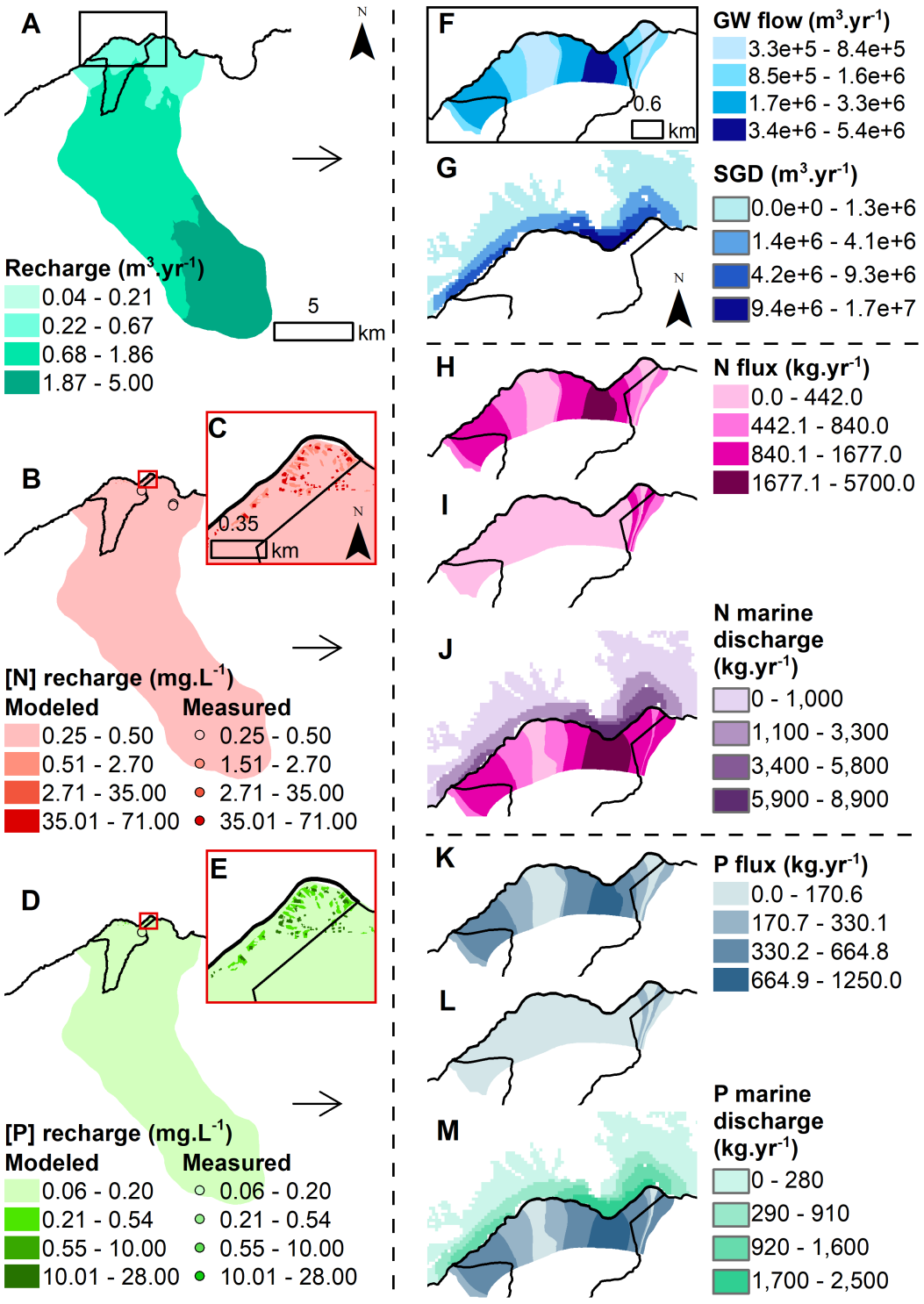

Fig 4. Groundwater recharge, associated nutrient concentrations, and groundwater discharge flux (i.e. terrestrial drivers) at Hā'ena. (A) Groundwater recharge ($m^3.yr^{-1}$). (B) Groundwater recharge N concentration ($mg.L^{-1}$) (with enlarged inset C). (D) Groundwater recharge P concentration ($mg.L^{-1}$) (with enlarged inset E). The modeled recharge (B) N and (D) P nutrient concentrations maps are overlaid with the GW survey points using the same color ramp for visual comparison. (F) Modeled coastal groundwater flow ($m^3.yr^{-1}$) coupled with (G) the SGD ($m^3.yr^{-1}$). (H) Background, (I) human-derived, and (J) total N flux ($kg.yr^{-1}$) by flow tube combined with N marine discharge plume ($kg.yr^{-1}$). (K) Background, (L) human-derived, and (M) total P flux ($kg.yr^{-1}$) by flow tube combined with P marine discharge plume ($kg.yr^{-1}$)The R^2 and p-value compare the measured N and P concentrations ($mg.L^{-1}$) in coastal waters and modeled (J) N and (M) P marine discharge ($kg.yr^{-1}$) (see S1 Fig for linear regressions).

https://doi.org/10.1371/journal.pone.0193230.g004

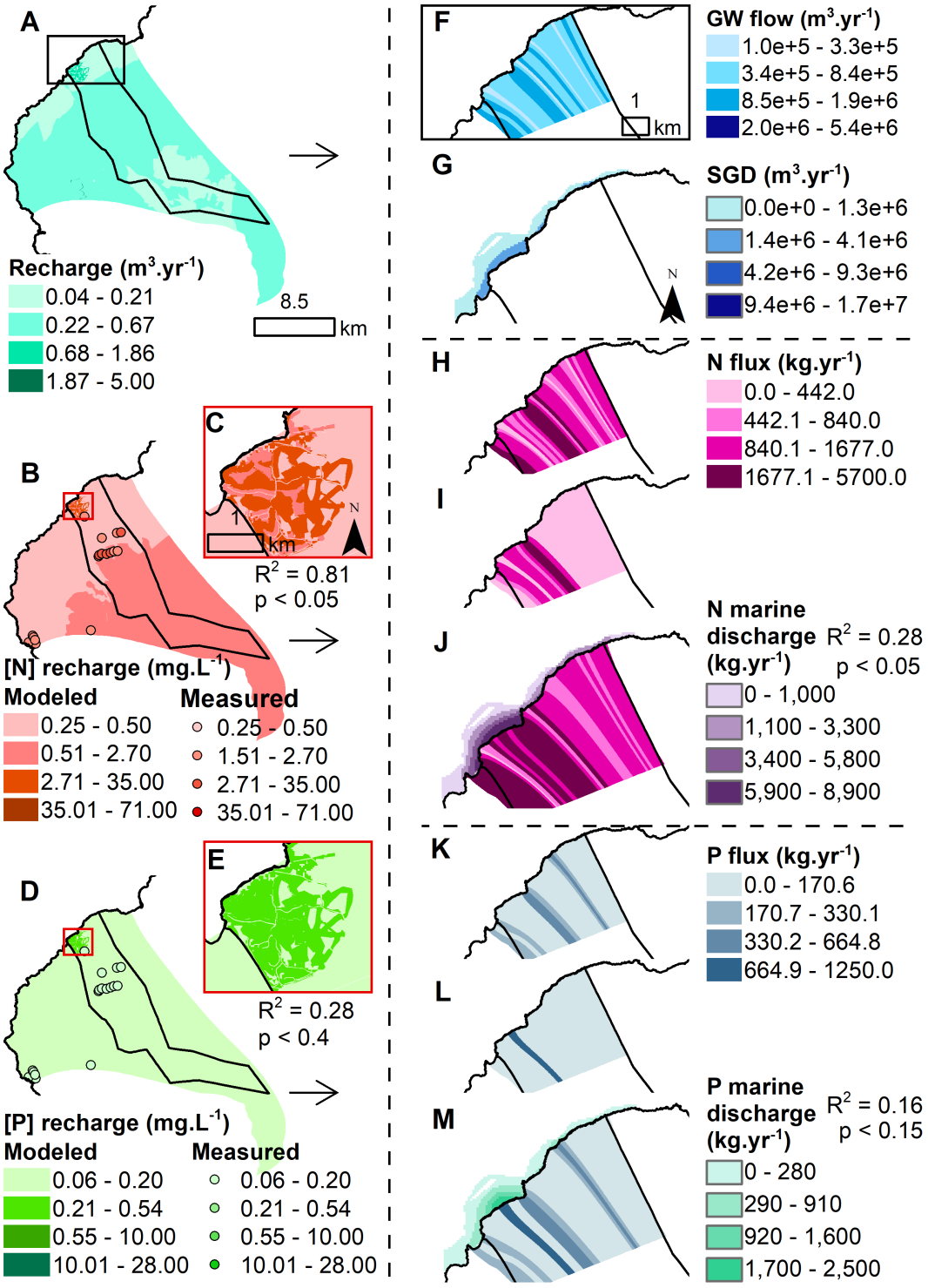

Fig 5. Groundwater recharge, associated nutrient concentrations, and groundwater discharge flux (i.e. terrestrial drivers) at Kaʻūpūlehu. (A) Groundwater recharge ($m^3.yr^{-1}$). (B) Groundwater recharge N concentration ($mg.L^{-1}$) (with enlarged inset C). (D) Groundwater recharge P concentration ($mg.L^{-1}$) (with enlarged inset E). The modeled recharge (B) N and (D) P nutrient concentrations maps are overlaid with the GW survey points using the same color ramp for visual comparison. The R^2 and p-value compare the measured and modeled (E) N and (I) P concentrations at Kaʻūpūlehu (see S1 Fig for linear regressions). (F) Modeled coastal groundwater flow ($m^3.yr^{-1}$) coupled with (G) the SGD ($m^3.yr^{-1}$). (H) Background, (I) human-derived, and (J) total N flux ($kg.yr^{-1}$) by flow tube combined with N marine discharge plume

(kg.yr^{-1}). (K) Background, (L) human-derived, and (M) total P flux (kg.yr^{-1}) by flow tube combined with P marine discharge plume (kg.yr^{-1})The R^2 and p-value compare the measured N and P concentrations (mg.L^{-1}) in coastal waters and modeled (J) N and (M) P marine discharge (kg.yr^{-1}) (see S1 Fig for linear regressions).

https://doi.org/10.1371/journal.pone.0193230.g005

In terms of habitat exposure, Hā'ena (Aspect $\bar{X} = 0.4 \pm 0.6$) was more exposed than Ka'ūpūlehu (Aspect $\bar{X} = 0.6 \pm 0.5$) (Fig 7I & 7J).

The second axis was also negatively correlated with the terrestrial drivers. It indicated that groundwater discharge (represented by freshwater) was higher at Hā'ena (57.1 million m^3.yr^{-1} or 10,279 m^3.m^{-1}.yr^{-1}) than Ka'ūpūlehu (22.7 million m^3.yr^{-1} or 3,085 m^3.m^{-1}.yr^{-1}), with higher input in bays at both sites (Figs 4F & 5F). Likewise, P flux was higher at Hā'ena (13,050 kg.yr^{-1} or 2.2 kg.yr^{-1}.m^{-1}), compared to Ka'ūpūlehu (6,760 kg.yr^{-1} or 0.8 kg.yr^{-1}.m^{-1}) (Figs 4M & 5M). Conversely, N flux was higher at Ka'ūpūlehu (55,540 kg.yr^{-1} or 7.1 kg.yr^{-1}.m^{-1}), in comparison to Hā'ena (36,320 kg.yr^{-1} or 6.0 kg.yr^{-1}.m^{-1}) (Figs 4G & 5G). The fraction of human-derived

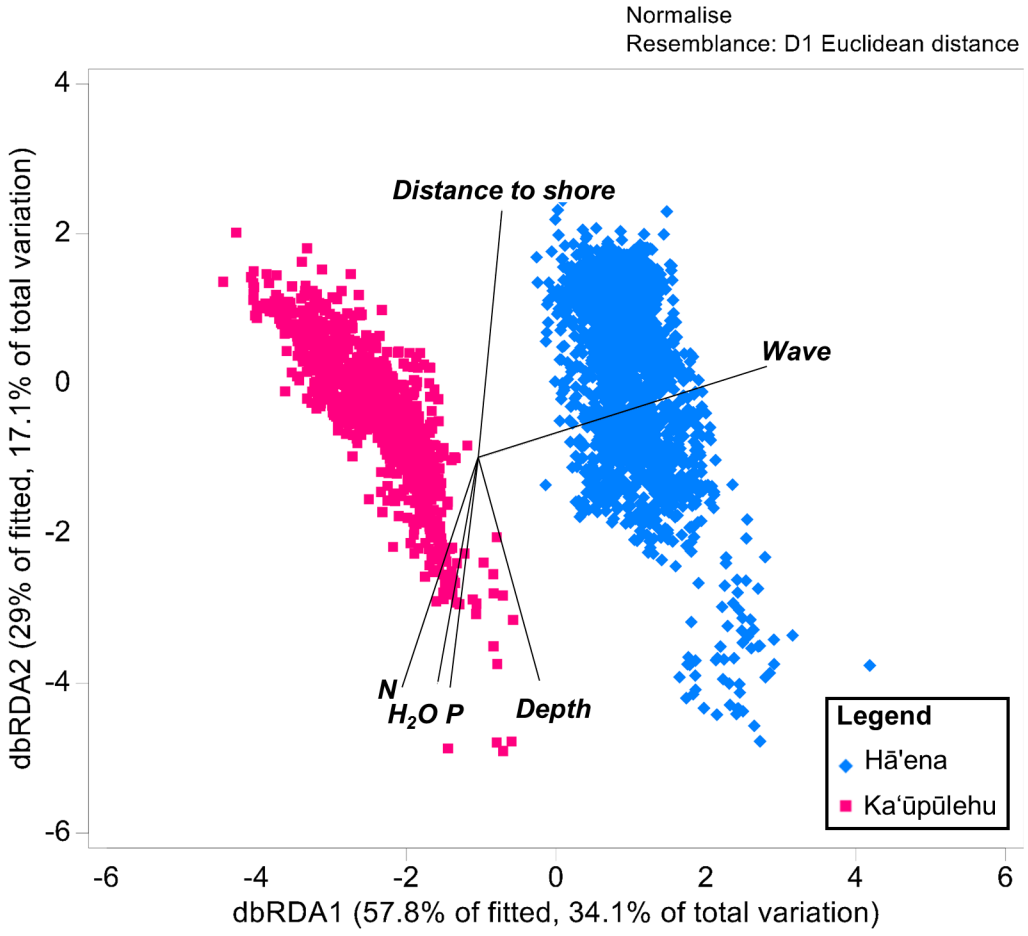

Fig 6. dbRDA of the coral reef communities. Ordination plot illustrating the relationship between terrestrial and marine drivers that best explain the variation of benthic and fish indicators in Hā'ena and Ka'ūpūlehu. The dbRDA vectors show the drivers explaining a significant proportion of the variation. The drivers differentiating the coral reef communities at Hā'ena from Ka'ūpūlehu are: wave power, distance to shore, depth, groundwater (H_2O) and nutrients (N and P).

https://doi.org/10.1371/journal.pone.0193230.g006

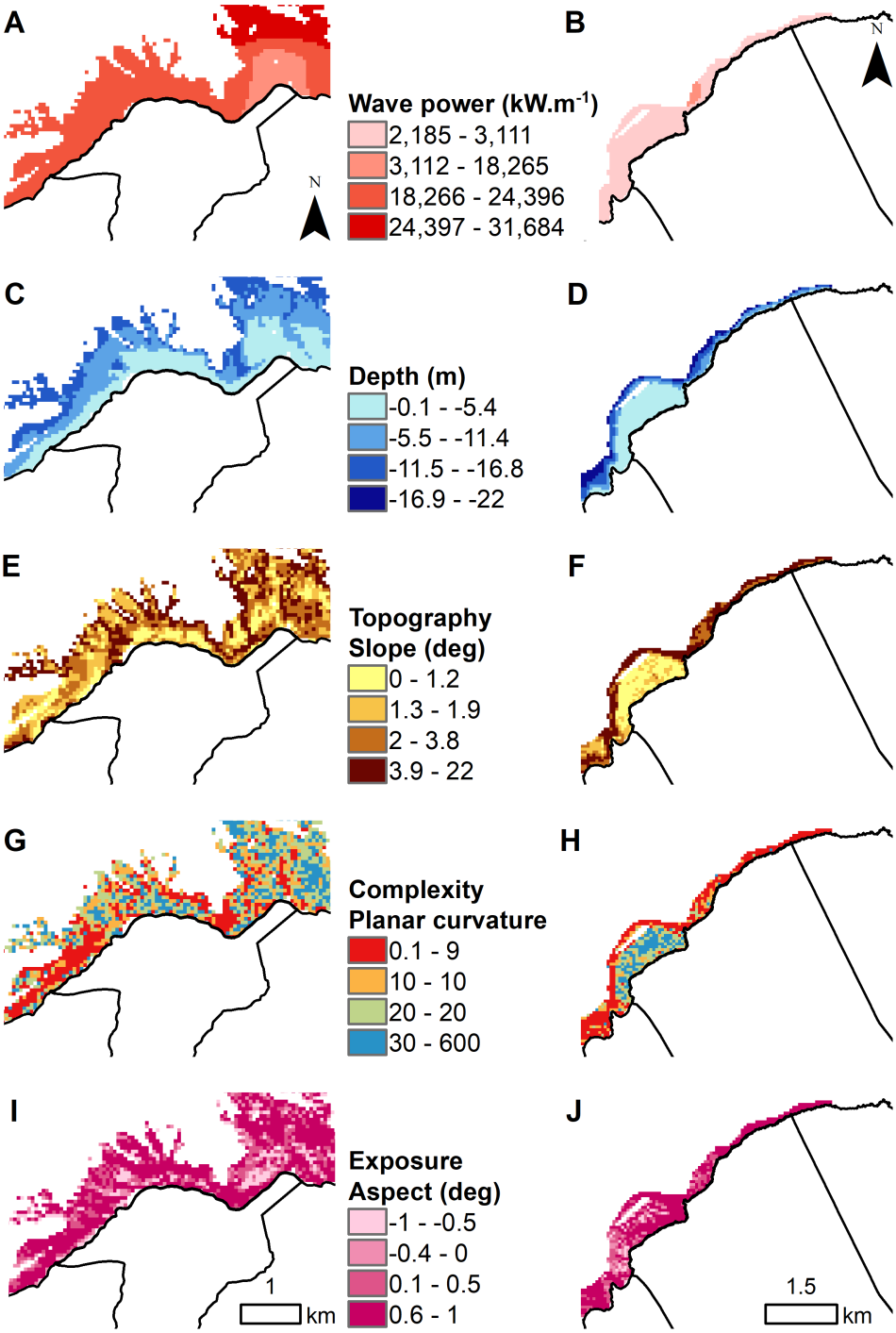

Fig 7. Marine drivers of coral reefs at Hā'ena and Ka'ūpūlehu. The marine drivers are represented by (A-B) wave power (kW.m^{-1}), (C-D) depth (m), (E-F) habitat topography (slope [degree]), (G-H) habitat complexity (planar curvature), and (I-J) habitat exposure (aspect [degree]) at Hā'ena and Ka'ūpūlehu, respectively.

https://doi.org/10.1371/journal.pone.0193230.g007

nutrient flux delivered to the coast was lower at Hā'ena (N = 16.4% and P = 10.7%) than Ka'ūpūlehu (N = 31.7% and P = 34.9%) (Figs 4I, 4L, 5I & 5L). In contrast, the fraction of natural-derived nutrient flux delivered to the coast was higher at Hā'ena (N = 83.6% and P = 89.3%) than Ka'ūpūlehu (N = 68.3% and P = 65.1%) (Figs 4H, 4K, 5H & 5K).

Coral reef models

The calibration and cross-validation of coral reef BRT models for Hā'ena explained 34–74% of the PDE and 10–51% of the CV PDE, respectively (S6 Table). At Ka'ūpūlehu, the calibration and cross-validation of coral reef models explained 21–60% of the PDE and 5–26% of the CV PDE, respectively. Analysis of the residuals from the final coral reef models showed no spatial autocorrelation (Moran's I Index $p > 0.1$). In terms of the terrestrial drivers, the coral reef models identified that groundwater discharge (represented by freshwater) was a key driver of coral reefs at Hā'ena, while nutrients played a more important role for coral reefs at Ka'ūpūlehu (Fig 8). At Hā'ena, freshwater had a negative effect on CCA, coral, and macroalgae, but was positively related to turf algae. Turf and macroalgae were weakly, yet positively related to N. Conversely, N had a negative effect on browser and piscivore biomass. At Ka'ūpūlehu, N had a negative effect on CCA, while P had a positive effect on turf algae and a negative effect on browsers. The effects of freshwater varied across fish indicators, as well as between sites.

In terms of the marine drivers, the coral reef models identified wave power, depth, and distance to shore as key drivers of coral reefs at Hā'ena (Fig 8). Wave power had a positive effect on CCA, macroalgae, and scrapers, but a negative effect on coral and turf algae. Coral was, however, positively associated with habitat exposure. CCA, coral, and most herbivores were positively associated with distance from shore, whereas turf and macroalgae showed a negative relationship. Depth had a negative effect on CCA and macroalgae. The fish indicators were more strongly associated with CCA, but scrapers were also negatively associated with macroalgae, while grazers positively associated with turf algae and coral. At Ka'ūpūlehu, the coral reef models identified habitat topography and complexity, as well as depth and distance to shore as key drivers of coral reefs (Fig 8). Although wave power had a positive effect on scraper and piscivore biomass, it had no effect on the benthic indicators. CCA and macroalgae were negatively related to distance to shore, whereas browsers and piscivores showed a positive relationship. The fish indicators were more strongly associated with coral and turf algae. Most benthic and fish indicators were positively associated with steeper, deeper reef slopes and more complex habitat, except for turf algae and browsers, which were negatively associated with habitat topography.

Coral reef predictive maps

Based on the key drivers and their relationship with the coral reef indicators at Hā'ena (i.e., freshwater, wave power, depth, and distance to shore) (Fig 8), the coral reef models predicted a benthic community with high CCA cover, particularly along the wave-exposed fore-reefs away from freshwater influence; higher coral cover was restricted to the sheltered back-reef areas; higher macroalgae was concentrated in the nearshore areas, close to sources of nutrients; while turf algae was high and more widespread (Fig 9). The coral reef models predicted a fish community with many grazers but few browsers, scrapers, and piscivores, with higher biomass for all indicators in more complex habitat, deeper waters, and away from the shore (Fig 9). Based on the comparison with the empirical surveys with the spatial predictions, all the indicators, except for the piscivores, showed a statistically significant relationship (Fig 9). The R^2 was higher for CCA and coral predictions compared to the turf and macroalgae predictions, and the grazers and scrapers predictions performed better than the browsers and piscivores. Those trends were consistent with their relative empirical abundance and biomass at the survey sites (Fig 9).

Based on the key drivers and their relationship with the coral reef indicators at Ka'ūpūlehu (i.e., nutrients, habitat topography and complexity, depth, and distance to shore) (Fig 8), the coral reef models predicted a benthic community with low CCA cover,

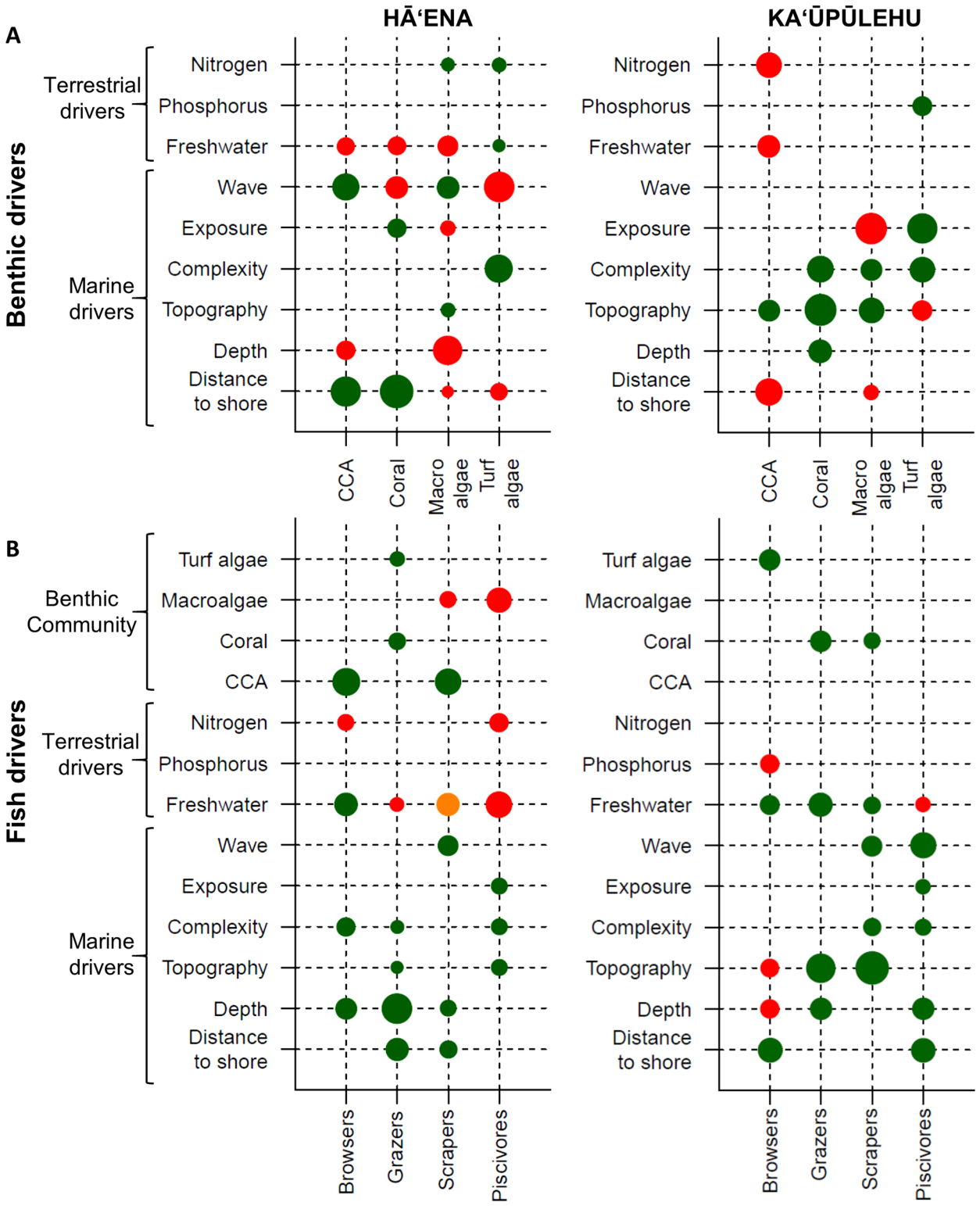

Fig 8. Coral reef predictive models. (A) Benthic and (B) fish predictive models for each site. The benthic and fish indicators are represented along the X axes. The terrestrial and marine drivers, and benthic community (for the fish models) are represented on the Y axes. The marine drivers include metrics related to wave power, habitat exposure, complexity, topography, and local geography (depth and distance to shore). The bubble size represents the relative percent contribution of each driver and the color indicates whether the relationship between the indicator and the driver is positive (green), concave/convex (yellow), or negative (red). Refer to S2–S7 Figs for more details on these relationships.

https://doi.org/10.1371/journal.pone.0193230.g008

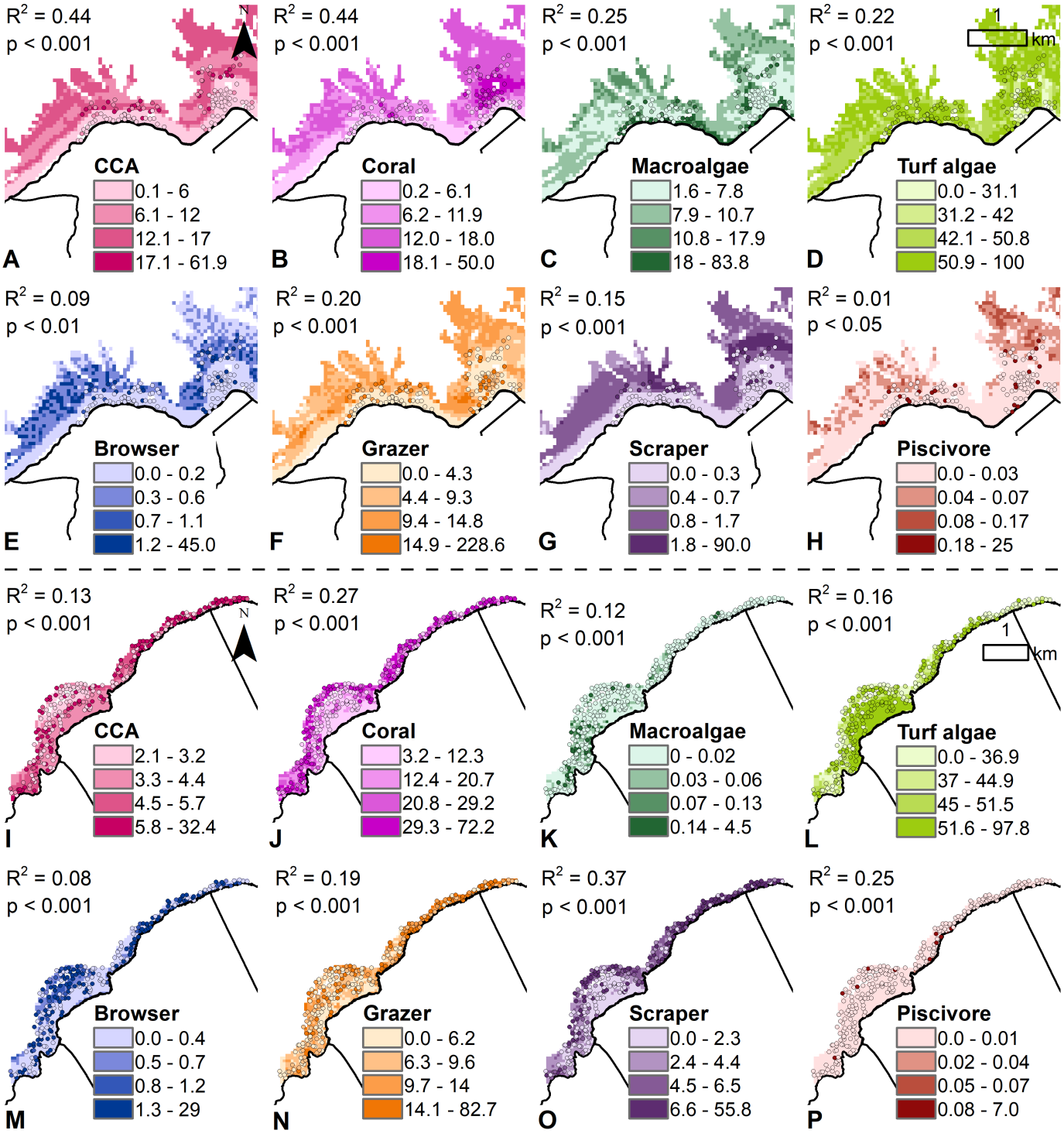

Fig 9. Observed and predicted distribution of coral reef indicators at Hā'ena and Ka'ūpūlehu. Benthic indicators at (A-D) Hā'ena and (I-L) Ka'ūpūlehu are measured in % cover and the fish indicators at (E-H) Hā'ena and (M-P) Ka'ūpūlehu are measured in $g.m^{-2}$. The predicted maps are overlaid with the survey points using the same color ramp for visual comparison, combined with the R^2 and p-values.

https://doi.org/10.1371/journal.pone.0193230.g009

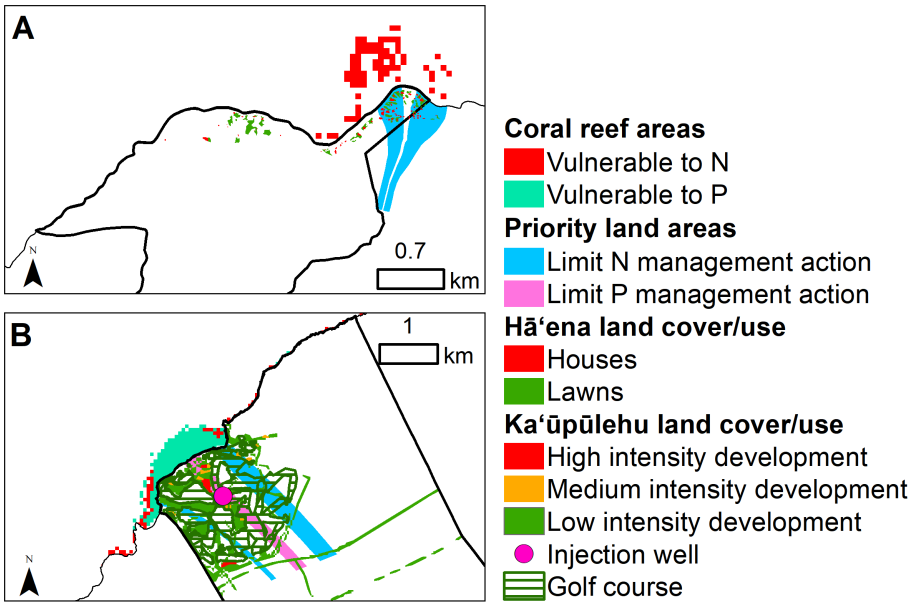

Fig 10. Coral reef areas vulnerable to land-based nutrients and priority land areas at Hā'ena and Ka'ūpūlehu. (A) Hā'ena and (B) Ka'ūpūlehu coral reef areas vulnerable to nutrients (N and P) combined with the priority land areas with the highest human derived nutrients and therefore, where management action should limit N and/or P inputs.

https://doi.org/10.1371/journal.pone.0193230.g010

restricted to the nearshore areas away from nutrient discharge; high coral cover, particularly along the reef slopes; low macroalgae cover restricted to the nearshore areas; and abundant turf algae cover on the reef flat, near nutrient discharge (Fig 9). The coral reef models predicted a fish community with many grazers and scrapers but few browsers and piscivores, with higher biomass for all indicators in more complex habitat, deeper waters, and away from the shore (Fig 9). Based on the comparison of the empirical surveys, the spatial predictions of all the indicators showed a statistically significant relationship (Fig 9). The R^2 was higher for coral and turf algae predictions compared to CCA and macroalgae predictions, and the scrapers and piscivore predictions performed better than the browsers and grazers. Those trends were also consistent with their relative empirical abundance and biomass at the survey sites (Fig 9).

Priority areas for management

By combining the selected criteria at Hā'ena, we found that the back-reef of Makua was vulnerable to nutrient inputs due to high exposure to N, limited wave mixing, and abundant benthic algae, as well coral bleaching due to high coral cover and shallow depth (Fig 10A). On land, the flow tubes located to the east of the site deliver the highest N flux. Based on the location of vulnerable coral reef areas, the cesspools located within these flow tubes should be prioritized for upgrade to septic systems. At Ka'ūpūlehu, we found that the coral reef areas more vulnerable to N input were located around the edges of existing development and along the reef slopes north of the development (Fig 10B). We also found that the reef flat located downstream from the development is more vulnerable to P input. On land, the flow tubes located to the north and south ends of the development, discharged the highest N flux in the small bays there, while the flow tubes located below the injection well discharged the highest P flux.

Discussion

To support ridge-to-reef management in high oceanic islands, this study developed a linked land-sea modeling framework that connects land cover/use to coral reefs through groundwater enriched nutrients at fine spatial resolution. We applied this framework in two *ahupua'a* subject to different natural disturbance regimes to compare and contrast the effects of terrestrial and marine drivers on coral reefs. Our results indicate that the terrestrial and marine drivers differed between sites due to their natural disturbance regimes and different island age. Hā'ena is primarily influenced by large-scale drivers (high rainfall and wave power), while Ka'ūpūlehu is mostly governed by local drivers (habitat and nutrients). Consistent with previous studies [22,130–132], our coral reef models showed that the high disturbance regime of Hā'ena has shaped a coral reef community dominated by CCA with cover of high turf algae and many grazers, while the low wave disturbance regime of Ka'ūpūlehu has allowed for the accretion of a coral dominated community with high turf and many grazers and scrapers. Similar to other studies [16,17,26,133–135], our coral reef predictive models showed that land-based nutrients can increase benthic algae, inhibit reef calcifiers (CCA), and decrease the biomass of locally important fishes. This study shows how coral reefs can differ under the influence of different natural disturbance regimes combined with local-scale terrestrial and marine drivers, thereby reinforcing the need for place-based ridge-to-reef management.

Groundwater as the land-sea linkage

Our groundwater flow modeling results reflected the rainfall patterns from each site, where recharge at Hā'ena was much higher than at Ka'ūpūlehu, and resulted in larger SGD in embayments [37,136]. Given that nutrient concentrations in groundwater depend on rates of recharge, the higher rates of recharge at Hā'ena resulted in more dilution and lower N concentrations, compared to Ka'ūpūlehu [137]. Our coastal nutrient flux discharge modeling results confirmed that groundwater at Ka'ūpūlehu has high natural N flux, despite the existing land cover consisting only of barren rock, shrubland, and native and invasive forests [138]. Some have hypothesized that the groundwater may be geothermally altered, but the exact source of N remains unknown [78,138]. Ka'ūpūlehu results were consistent with other areas on the dry leeward side of Hawai'i Island, where coastal groundwater nutrient fluxes are high (e.g., N:2,000 and P: 200 $kg.ha^{-1}.yr^{-1}$), compared to other less dry high latitude oceanic islands, such as South Korea (N:1,100 and P:20 $kg.ha^{-1}.yr^{-1}$) [59,139]. Hā'ena nutrient flux modeling results were consistent with other wet and rural *ahupua'a* along the Main Hawaiian Islands chain, such as Hanalei on the windward side of Kaua'i, Kahana on the windward side of O'ahu, and the south shore of Moloka'i [59,62,107]. At Hā'ena, a large fraction of the total nutrient flux is derived from natural processes due to abundant rainfall. Because we assumed constant background nutrient concentrations, the higher groundwater discharge rates resulted in higher background nutrient flux. Similar to other studies [60,61,140], our results indicated that SGD on oceanic islands can be a primary vector for land-based nutrients to coral reefs.

Anthropogenic sources of nutrients

This study showed that wastewater disposal via cesspools at Hā'ena was the major source of human-derived nutrients. The impact of sewage discharge on coral reefs has been recognized as a major environmental problem in Hawai'i [103,141], as well as in regions such as Reunion and Mauritius [122], the Red Sea [142], Florida Keys [143], and the Great Barrier Reef [144]. While, revised wastewater regulations declared a statewide ban of new cesspools in Hawai'i in 2016 (HAR Title 11, Chapter 62), they currently represent the most prevalent wastewater

disposal system across the main Hawaiian Islands (e.g., 76% and 84% of the OSDS currently used on Kauaʻi and Hawaiʻi Island, respectively) [145], and have been recognized as a primary driver of groundwater and nearshore water quality degradation [146]. At Kaʻūpūlehu, we identified the golf course and injection well as the major sources of nutrients. Studies elsewhere in Hawaiʻi have also shown that nutrient concentrations can be significantly higher in proximity to golf courses [60,106,147].

Effect of SGD on coral reefs

Freshwater input from SGD can reduce salinity in shallow waters [15,60,89]. Higher freshwater input at Hāʻena played an important role in structuring coral reefs. Consistent with their ecology and salinity tolerance [15,148,149], CCA and coral cover were lower near high freshwater inputs. Conversely, decreases in salinity have been shown to directly promote turf algae growth or indirectly hinder competition for space by other species [150]. Freshwater input had a mixed effect on the distribution of the fish indicators, which may be due to the fact that fishes are mobile and tolerate a wider range of salinity, which varies among species [151]. The ecological responses of turf, and macroalgae to nutrients suggested that Hāʻena may be N-limited, as was shown in nearby Hanalei Bay [106], while Kaʻūpūlehu may be P-limited, as was found in Honokōhau Bay, also located on the leeward side of Hawaiʻi Island [58]. Vermeij et al. [134] showed that local nutrient enrichment can foster turf algae overgrowth and reduce CCA and coral recovery after disturbances, through loss of space availability [152]. Similarly, our results showed that macroalgae, but especially turf algae, may have a competitive advantage over corals and CCA under a future scenario of land-based nutrient increase in nearshore waters, particularly at Kaʻūpūlehu and the back-reefs of Hāʻena. Naturally more dominant and competitive under the higher wave disturbance regime in the central Pacific region [22,67,132], turf algae can proliferate rapidly and lead to phase shifts when exposed to land-based nutrients [16,17,26]. Consistent with their ecological role, grazers at Hāʻena and browsers at Kaʻūpūlehu appear to be controlling turf algae, demonstrating their importance for coral reef resilience [16,17,20].

Effect of wave power on coral reefs

On Hawaiian reefs, wave power is a key driver controlling coral growth, reef development, and the structure of coral reef communities [22,131,153]. CCA has been found to be more dominant and competitive under high wave disturbance regimes on coral reefs in the central Pacific region [22,67,132]. The coral and CCA abundance patterns at both sites indicated that CCA may be out-competed by coral under low wave conditions suited to coral growth, but flourish in high wave conditions adverse to coral growth [130,154,155]. Exposed to high wave power, the benthic community on the fore-reefs at Hāʻena is dominated by CCA, while coral growth is primarily restricted to the sheltered back-reef of Makua. By contrast, coral growth at Kaʻūpūlehu was more widespread across the reef slope. The effect of wave disturbance on fish populations is not well studied, due to the challenges of conducting field work in high wave environments [156–158]. Our results suggest that fishes may benefit from reduced access due to localized wave action at both sites, implying that wave power provides protection from fishing pressure [156,159,160]. These patterns have been observed elsewhere across the Hawaiian Archipelago, where coral reefs in wave exposed settings are often suppressed to a thin veneer and support high fish biomass, while coral reefs in sheltered areas have accreted slowly over time and support lower fish biomass [22,159,161].

Effect of habitat on coral reefs

Owing to their island age coupled with their natural disturbance regimes, coral reef habitats at Hāʻena and Kaʻūpūlehu exhibit different topographies and complexities. Coral reefs on young islands form relatively narrow fringes, such as in Kaʻūpūlehu, while coral reefs around older islands, form wider and shallower reef flats, such as in Hāʻena [153]. Many studies have shown that habitat topography and complexity are primary drivers controlling coral reefs [130,158,159,162], as shown in Kaʻūpūlehu, compared to Hāʻena where on habitat topography and complexity were less important. At Kaʻūpūlehu, CCA, coral cover, and fish biomass were generally high along the reef slopes, while turf and macroalgae cover was higher on the reef flats. Our results show that local-scale habitat characteristics played an important role in shaping these coral reefs, which was emphasized in the low natural disturbance regime at Kaʻūpūlehu.

Management implications

At first glance, Kaʻūpūlehu is more susceptible to nutrient inputs from coastal development and coral bleaching due to high levels of background N in groundwater, combined with limited dilution and mixing from low rainfall and wave power, and high coral and turf algae cover. Based on the location of the vulnerable coral reef areas, our results suggest monitoring the effect of N discharge from the flow tubes located upslope from Uluweuweu and Kahuwai bays and P discharge from the central flow tube beneath the injection well. Currently, Hāʻena is rural with limited development or agriculture, therefore most of the nutrient discharge comes from natural processes, with the exception of land areas to the east of the *ahupuaʻa* where nutrient discharge is largely human-derived. Although Hāʻena benefits from mixing and dilution due to high freshwater and wave power, the back-reef areas are shallow, sheltered from waves, exposed to natural and human-derived nutrients, and support high coral and algae cover. For these reasons, the back-reef areas of Hāʻena are expected to be more vulnerable to coral bleaching and algae overgrowth due to nutrient inputs from existing and future coastal development.

The communities in both places have initiated the protection of herbivores, through marine closures, which can offset some of the effects of nutrients by controlling algae cover [16,17,163]. However, to ensure coral reef resilience in a changing climate, land-based nutrients inputs should also be addressed. Using this framework to inform resilience management through a ridge-to-reef approach, we identified priority areas on land where limiting nutrient inputs could prevent increase in benthic algae and promote chances of coral recovery post-bleaching impacts. At Hāʻena, management actions could focus on upgrading cesspools located upstream from Makua back-reef, which has been shown to be a nursery habitat or *Puʻuhonua* for fishes [71], and is protected as such under the management plan of the Community Based Subsistence Fisheries Management Area [164]. At Kaʻūpūlehu, management actions could focus on minimizing increase in P from the injection well discharge and that best management practices are employed for fertilizer application on green spaces located upstream from Uluweuweu bay and Kahuwai bay, which was identified by the Kaʻūpūlehu community to contain a groundwater spring (*Wai a Kāne*) of cultural and historical importance [165].

Limitations and future research

Given that this framework was calibrated on existing data, some models could not be validated, or only partially validated, due to limited or lack of data. At Hāʻena, the groundwater model was parametrized with limited groundwater samples and the coastal discharge models could

not be validated due to lack of coastal water quality data. At Kaʻūpūlehu, the coastal discharge models were partially ground-truthed due to limited coastal water quality data. In addition, we used existing wave data to represent mixing effect from wave action on the diffusion of the SGD, given circulation data was not available for our study sites. To strengthen this method, future work using this approach should include groundwater sampling with SGD measurements, incorporate nearshore circulation information, and couple coral reef surveying with water quality sampling. Thus more refined groundwater models and reliable maps of coastal water quality could be generated. Additionally, our predictive coral reef models were calibrated on contemporary data sets and the derived relationships (response curves) should be further compared against historical data trends for validation. Although this framework was developed based on limited water quality data, we had access to comprehensive datasets for the coral reef models. This allowed us to ground-truth the predicted maps of our resilience indicators, which were the final output of the modeling framework.

Species composition and relative abundance can affect the predictability of selected indicators [166], as illustrated by the differences in observed abundance of CCA and coral between with our study sites. However, the same coral reef survey methods were used to record benthic and fish data at both sites, thus eliminating a potential source of bias. To improve the predictions of the coral reef models, future research in those locations should couple coral reef surveys with water quality and oceanographic conditions (e.g., waves or currents). In light of these caveats, these priority areas should be seen as target zones for wastewater management and further investigation of land-sea impacts. Because these models were developed at high spatial resolution in places where communities are stewards of the environment, we leveraged input from local community members and their observations to further ground-truth our maps and priority areas. The fact that the areas identified as vulnerable coincided with local observations from community members provided additional confidence to our recommendations.

Conclusions

Managers need spatially-explicit place-based models to better understand the impact of anthropogenic drivers on coral reefs and manage them more effectively. Empirical data provide point data at the location of the survey, but do not provide a continuous surface to support spatial prioritization of management actions [167]. Tools that provide visualization and quantify potential impacts are needed to better manage coral reefs [11,168]. The linked land-sea modeling framework presented here can help managers evaluate the spatial variation and influence of terrestrial and marine drivers, mediated by anthropogenic activities, on coral reefs, and prioritize management actions accordingly. Although these linked land-sea models were built to understand the land-sea linkages specific to these places, many of the processes, ecological effects, and management actions, we described can be generalized to other oceanic island environments comprised within this spectrum of natural disturbance regimes. Additionally, when calibrated for a place and assuming the fundamental ecological relationships are constant over time, this framework can be used to forecast and assess indicator distributions based on land cover/use change, marine closures, and climate change scenarios.

Supporting information

S1 File. Copyright permission Charles Fletcher.
(PDF)

S1 Table. Modeling framework response variables description. Benthic (% cover) and fish biomass ($g.m^{-1}$) coral reef indicators were derived from the coral reef surveys and used as response variables in the coral reef models.
(DOCX)

S2 Table. Fish species composition per functional groups.
(DOCX)

S3 Table. Coastal water quality data at Kaʻūpūlehu. See Carlson and Wiegner [169] for more details on sample collection, processing, and analytical methods.
(DOCX)

S4 Table. Response variables and drivers' relationships. This table provides the hypothesized relationships between the drivers and coral reef indicators.
(DOCX)

S5 Table. Modeling framework predictor variables description and processing methods. This table provides a description of all the predictor variables modeled in the coral reef models. Each metric is classified by type (terrestrial drivers or marine drivers) and assigned a code for modeling. The table below indicates the data source and analytical tool used to generate each metric. Refer to Stamoulis & Delevaux et al. [110] for more details on processing methods.
(DOCX)

S6 Table. Coral reef predictive model performance per indicator. The percent deviance explained (PDE) by the BRT models for the calibration and cross-validation (CV) processes and the final number of predictors (Xi) is shown for Hāʻena and Kaʻūpūlehu.
(DOCX)

S1 Fig. Measured versus modeled nutrients for groundwater and coastal discharge at Kaʻūpūlehu.
(TIFF)

S2 Fig. Response curves of the benthic indicators at Hāʻena.
(TIF)

S3 Fig. Response curves of the herbivore fish indicators at Hāʻena.
(TIF)

S4 Fig. Response curves of the piscivore fish indicators at Hāʻena.
(TIF)

S5 Fig. Response curves of benthic indicators at Kaʻūpūlehu.
(TIF)

S6 Fig. Response curves of herbivore fish indicators at Kaʻūpūlehu.
(TIF)

S7 Fig. Response curves of piscivore fish indicators at Kaʻūpūlehu.
(TIF)

S8 Fig. Observed versus predicted coral reef indicators at Hāʻena.
(TIF)

S9 Fig. Observed versus predicted coral reef indicators at Kaʻūpūlehu.
(TIF)

Acknowledgments

The views expressed in this article are those of the authors and do not necessarily reflect the views or policies of their respective agencies (EPA, NOAA, WCS, TNC, NGS, KS, and NTBG). The authors would like to thank the department of Natural Resources and Environmental Management at the University of Hawai'i, and particularly Peter Garrod for his mentorship and making this work possible. We would like to also acknowledge Daniel Amato from the Department of Botany, Jonatha Giddens from the Department of Biology at the University of Hawai'i, and Lida Teneva from Hawai'i Conservation International for reviewing earlier drafts and providing key inputs throughout the development of this linked land-sea modeling framework. Lisa Mandle of the Natural Capital Project provided early input into the modeling framework. This work would have not been possible without technical support from key collaborators at the NOAA National Centers for Coastal Ocean Science, particularly Bryan Costa and Matt Kendall. The authors would like to also give recognition to Noa Lincoln from the Department of Tropical Plant and Soil Sciences at the University of Hawai'i and Kim Falinski from The Nature Conservancy, Hawaii Marine Program, for providing information on golf courses and associated nutrient loading rates. The authors are also grateful for Mehana Vaughan and her lab, who helped craft the story in its early stages. Thanks to Rebecca Most from The Nature Conservancy for mapping the 'Try Wait' boundaries at Ka'ūpūlehu. Finally, the authors would like to thank the communities of Hā'ena and Ka'ūpūlehu for inspiring this work and providing guidance and feedback on the research outputs.

Author Contributions

Conceptualization: Jade M. S. Delevaux, Robert Whittier, Kostantinos A. Stamoulis, Leah L. Bremer, Stacy Jupiter, Alan M. Friedlander, Kawika B. Winter, Robert Toonen, Kimberly Burnett, Tamara Ticktin.

Data curation: Jade M. S. Delevaux, Robert Whittier, Kostantinos A. Stamoulis, Matthew Poti.

Formal analysis: Jade M. S. Delevaux, Robert Whittier, Anders Knudby.

Funding acquisition: Jade M. S. Delevaux, Stacy Jupiter, Alan M. Friedlander, Kimberly Burnett, Kirsten L. L. Oleson, Tamara Ticktin.

Investigation: Jade M. S. Delevaux, Robert Whittier, Kostantinos A. Stamoulis, Natalie Kurashima, Eric Conklin, Chad Wiggins, Whitney Goodell, Tracy Wiegner.

Methodology: Jade M. S. Delevaux, Robert Whittier, Kostantinos A. Stamoulis, Leah L. Bremer, Stacy Jupiter, Alan M. Friedlander, Robert Toonen, Susan Yee, Tamara Ticktin.

Project administration: Jade M. S. Delevaux, Leah L. Bremer, Tamara Ticktin.

Resources: Jade M. S. Delevaux, Robert Whittier, Leah L. Bremer, Stacy Jupiter, Alan M. Friedlander, Greg Guannel, Hla Htun, Tamara Ticktin.

Software: Jade M. S. Delevaux, Robert Whittier, Alan M. Friedlander, Matthew Poti, Tamara Ticktin.

Supervision: Jade M. S. Delevaux, Leah L. Bremer, Stacy Jupiter, Alan M. Friedlander, Greg Guannel, Kawika B. Winter, Tamara Ticktin.

Validation: Jade M. S. Delevaux, Robert Whittier, Kostantinos A. Stamoulis, Leah L. Bremer, Stacy Jupiter, Alan M. Friedlander, Matthew Poti, Kawika B. Winter.

Visualization: Jade M. S. Delevaux, Robert Whittier, Kostantinos A. Stamoulis.

Writing – original draft: Jade M. S. Delevaux, Robert Whittier.

Writing – review & editing: Jade M. S. Delevaux, Robert Whittier, Kostantinos A. Stamoulis, Leah L. Bremer, Stacy Jupiter, Alan M. Friedlander, Matthew Poti, Greg Guannel, Natalie Kurashima, Kawika B. Winter, Robert Toonen, Eric Conklin, Chad Wiggins, Anders Knudby, Whitney Goodell, Kimberly Burnett, Susan Yee, Hla Htun, Kirsten L. L. Oleson, Tracy Wiegner, Tamara Ticktin.

References

1. Webster PJ, Holland GJ, Curry JA, Chang H-R. Changes in tropical cyclone number, duration, and intensity in a warming environment. Science. 2005; 309: 1844–1846. https://doi.org/10.1126/science.1116448 PMID: 16166514
2. Hoegh-Guldberg O, Mumby PJ, Hooten AJ, Steneck RS, Greenfield P, Gomez E, et al. Coral reefs under rapid climate change and ocean acidification. science. 2007; 318: 1737–1742. https://doi.org/10.1126/science.1152509 PMID: 18079392
3. Hoegh-Guldberg O. Climate change, coral bleaching and the future of the world's coral reefs. Mar Freshw Res. 1999; 50: 839–866.
4. Nyström M, Folke C, Moberg F. Coral reef disturbance and resilience in a human-dominated environment. Trends Ecol Evol. 2000; 15: 413–417. https://doi.org/10.1016/S0169-5347(00)01948-0 PMID: 10998519
5. Hughes TP, Graham NAJ, Jackson JBC, Mumby PJ, Steneck RS. Rising to the challenge of sustaining coral reef resilience. Trends Ecol Evol. 2010; 25: 633–642. https://doi.org/10.1016/j.tree.2010.07.011 PMID: 20800316
6. Moberg F, Folke C. Ecological goods and services of coral reef ecosystems. Ecol Econ. 1999; 29: 215–233.
7. Worm B, Barbier EB, Beaumont N, Duffy JE, Folke C, Halpern BS, et al. Impacts of biodiversity loss on ocean ecosystem services. science. 2006; 314: 787–790. https://doi.org/10.1126/science.1132294 PMID: 17082450
8. Morecroft MD, Crick HQ, Duffield SJ, Macgregor NA. Resilience to climate change: translating principles into practice. J Appl Ecol. 2012; 49: 547–551.
9. Holling CS. Resilience and stability of ecological systems. Annu Rev Ecol Syst. 1973; 4: 1–23.
10. Bridge TCL, Hughes TP, Guinotte JM, Bongaerts P. Call to protect all coral reefs. Nat Clim Change. 2013; 3: 528–530. https://doi.org/10.1038/nclimate1879
11. Gurney GG, Melbourne-Thomas J, Geronimo RC, Aliño PM, Johnson CR. Modelling Coral Reef Futures to Inform Management: Can Reducing Local-Scale Stressors Conserve Reefs under Climate Change? PLOS ONE. 2013; 8: e80137. https://doi.org/10.1371/journal.pone.0080137 PMID: 24260347
12. Pickett STA, White PS, editors. The Ecology of Natural Disturbance and Patch Dynamics [Internet]. San Diego: Academic Press; 1985. https://doi.org/10.1016/B978-0-12-554520-4.50002-2
13. Jackson JB. Adaptation and diversity of reef corals. BioScience. 1991; 475–482.
14. Brown CJ, Saunders MI, Possingham HP, Richardson AJ. Managing for interactions between local and global stressors of ecosystems. PloS One. 2013; 8: e65765. https://doi.org/10.1371/journal.pone.0065765 PMID: 23776542
15. Jokiel PL, Hunter CL, Taguchi S, Watarai L. Ecological impact of a fresh-water "reef kill" in Kaneohe Bay, Oahu, Hawaii. Coral Reefs. 1993; 12: 177–184. https://doi.org/10.1007/BF00334477
16. Smith JE, Hunter CL, Smith CM. The effects of top–down versus bottom–up control on benthic coral reef community structure. Oecologia. 2010; 163: 497–507. https://doi.org/10.1007/s00442-009-1546-z PMID: 20058024
17. Littler MM, Littler DS, Brooks BL. Harmful algae on tropical coral reefs: Bottom-up eutrophication and top-down herbivory. Harmful Algae. 2006; 5: 565–585. https://doi.org/10.1016/j.hal.2005.11.003
18. Jackson JB, Kirby MX, Berger WH, Bjorndal KA, Botsford LW, Bourque BJ, et al. Historical overfishing and the recent collapse of coastal ecosystems. science. 2001; 293: 629–637. https://doi.org/10.1126/science.1059199 PMID: 11474098
19. Edwards CB, Friedlander AM, Green AG, Hardt MJ, Sala E, Sweatman HP, et al. Global assessment of the status of coral reef herbivorous fishes: evidence for fishing effects. Proc R Soc Lond B Biol Sci. 2014; 281: 20131835.

20. Green AL, Bellwood DR. Monitoring functional groups of herbivorous reef fishes as indicators of coral reef resilience: a practical guide for coral reef managers in the Asia Pacific region. IUCN; 2009.
21. Done TJ. Coral Community Adaptability to Environmental Change at the Scales of Regions, Reefs and Reef Zones. Integr Comp Biol. 1999; 39: 66–79. https://doi.org/10.1093/icb/39.1.66
22. Dollar SJ. Wave stress and coral community structure in Hawaii. Coral Reefs. 1982; 1: 71–81. https://doi.org/10.1007/BF00301688
23. Grigg RW. Community structure, succession and development of coral reefs in Hawaii. Mar Ecol Prog Ser. 1983; 11: 1–14.
24. Hughes TP, Connell JH. Multiple stressors on coral reefs: A long -term perspective. Limnol Oceanogr. 1999; 44: 932–940. https://doi.org/10.4319/lo.1999.44.3_part_2.0932
25. Sebens KP. Habitat structure and community dynamics in marine benthic systems. In: Bell SS, McCoy ED, Mushinsky HR, editors. Habitat Structure. Springer Netherlands; 1991. pp. 211–234. https://doi.org/10.1007/978-94-011-3076-9_11
26. Fabricius KE. Effects of terrestrial runoff on the ecology of corals and coral reefs: review and synthesis. Mar Pollut Bull. 2005; 50: 125–146. https://doi.org/10.1016/j.marpolbul.2004.11.028 PMID: 15737355
27. Kubicek A, Muhando C, Reuter H. Simulations of Long-Term Community Dynamics in Coral Reefs—How Perturbations Shape Trajectories. PLOS Comput Biol. 2012; 8: e1002791. https://doi.org/10.1371/journal.pcbi.1002791 PMID: 23209397
28. Bartley R, Bainbridge ZT, Lewis SE, Kroon FJ, Wilkinson SN, Brodie JE, et al. Relating sediment impacts on coral reefs to watershed sources, processes and management: A review. Sci Total Environ. 2014; 468: 1138–1153. https://doi.org/10.1016/j.scitotenv.2013.09.030 PMID: 24121565
29. Risk MJ, Edinger E. Impacts of sediment on coral reefs. Encyclopedia of Modern Coral Reefs. Springer; 2011. pp. 575–586. http://link.springer.com/10.1007/978-90-481-2639-2_25
30. McGregor DP, Morelli P, Matsuoka J, Minerbi L, Becker HA, Vanclay F. An ecological model of well-being. Int Handb Soc Impact Assess Concept Methodol Adv. 2003; 109–126.
31. Minerbi L. Indigenous management models and protection of the ahupua 'a. Soc Process Hawai 'i. 1999; 39: 208–225.
32. Berkes F, Colding J, Folke C. Rediscovery of traditional ecological knowledge as adaptive management. Ecol Appl. 2000; 10: 1251–1262.
33. Johannes RE. The renaissance of community-based marine resource management in Oceania. Annu Rev Ecol Syst. 2002; 33: 317–340.
34. Maris KA. Under what circumstances do people put unsustainable demands on island environments?: evidence from the North Atlantic [Internet]. University of Edinburgh. 2007. http://ethos.bl.uk/OrderDetails.do?uin=uk.bl.ethos.657316
35. Jupiter SD, Wenger A, Klein CJ, Albert S, Mangubhai S, Nelson J, et al. Opportunities and constraints for implementing integrated land–sea management on islands. Environ Conserv. 2017; 1–13.
36. Neall VE, Trewick SA. The age and origin of the Pacific islands: a geological overview. Philos Trans R Soc B Biol Sci. 2008; 363: 3293–3308. https://doi.org/10.1098/rstb.2008.0119 PMID: 18768382
37. Giambelluca TW, Chen Q, Frazier AG, Price JP, Chen Y-L, Chu P-S, et al. Online Rainfall Atlas of Hawai'i. Bull Am Meteorol Soc. 2012; 94: 313–316. https://doi.org/10.1175/BAMS-D-11-00228.1
38. Giambelluca TW, Shuai X, Barnes ML, Alliss RJ, Longman RJ, Miura T, et al. Evapotranspiration of Hawai'i. U.S. Army Corps of Engineers—Honolulu District, and the Commission on Water Resource Management, State of Hawai'i.; 2014.
39. Moberly R Jr, Baver LD Jr, Morrison A. Source and variation of Hawaiian littoral sand. J Sediment Res. 1965; 35. Available: http://archives.datapages.com/data/sepm/journals/v33-37/data/035/035003/0589.htm
40. Gove JM, Williams GJ, McManus MA, Heron SF, Sandin SA, Vetter OJ, et al. Quantifying climatological ranges and anomalies for Pacific coral reef ecosystems. PloS One. 2013; 8: e61974. https://doi.org/10.1371/journal.pone.0061974 PMID: 23637939
41. Buma B. Disturbance interactions: characterization, prediction, and the potential for cascading effects. Ecosphere. 2015; 6: 1–15. https://doi.org/10.1890/ES15-00058.1
42. Adjeroud M, Michonneau F, Edmunds PJ, Chancerelle Y, Penin L, Vidal-Dupiol J, et al. Recurrent large-scale disturbances, recovery trajectories, and resilience of coral assemblages on a coral reef in the south-central Pacific. 2008. https://hal.archives-ouvertes.fr/halsde-00332281
43. Chabanet P, Adjeroud M, Andréfouët S, Bozec Y-M, Ferraris J, Garcìa-Charton J-A, et al. Human-induced physical disturbances and their indicators on coral reef habitats: A multi-scale approach. Aquat Living Resour. 2005; 18: 215–230. https://doi.org/10.1051/alr:2005028

44. Hughes TP, Baird AH, Dinsdale EA, Harriott VJ, Moltschaniwskyj NA, Pratchett MS, et al. Detecting Regional Variation Using Meta-Analysis and Large-Scale Sampling: Latitudinal Patterns in Recruitment. Ecology. 2002; 83: 436–451. https://doi.org/10.1890/0012-9658(2002)083[0436:DRVUMA]2.0.CO;2

45. Connell JH. Disturbance and recovery of coral assemblages. Coral Reefs. 1997; 16: S101–S113. https://doi.org/10.1007/s003380050246

46. Kouwen FV, Dieperink C, Schot P, Wassen M. Applicability of Decision Support Systems for Integrated Coastal Zone Management. Coast Manag. 2007; 36: 19–34. https://doi.org/10.1080/08920750701682007

47. Klein CJ, Ban NC, Halpern BS, Beger M, Game ET, Grantham HS, et al. Prioritizing land and sea conservation investments to protect coral reefs. PLoS One. 2010; 5: e12431. https://doi.org/10.1371/journal.pone.0012431 PMID: 20814570

48. Jenkins AP, Jupiter SD, Qauqau I, Atherton J. The importance of ecosystem-based management for conserving aquatic migratory pathways on tropical high islands: a case study from Fiji. Aquat Conserv Mar Freshw Ecosyst. 2010; 20: 224–238.

49. Halpern BS, Walbridge S, Selkoe KA, Kappel CV, Micheli F, D'Agrosa C, et al. A Global Map of Human Impact on Marine Ecosystems. Science. 2008; 319: 948–952. https://doi.org/10.1126/science.1149345 PMID: 18276889

50. Klein CJ, Jupiter SD, Selig ER, Watts ME, Halpern BS, Kamal M, et al. Forest conservation delivers highly variable coral reef conservation outcomes. Ecol Appl. 2012; 22: 1246–1256. PMID: 22827132

51. Tulloch VJ, Brown CJ, Possingham HP, Jupiter SD, Maina JM, Klein C. Improving conservation outcomes for coral reefs affected by future oil palm development in Papua New Guinea. Biol Conserv. 2016; 203: 43–54.

52. Tallis H, Ferdana Z, Gray E. Linking terrestrial and marine conservation planning and threats analysis. Conserv Biol. 2008; 22: 120–130. https://doi.org/10.1111/j.1523-1739.2007.00861.x PMID: 18254857

53. McClanahan TR. A coral reef ecosystem-fisheries model: impacts of fishing intensity and catch selection on reef structure and processes. Ecol Model. 1995; 80: 1–19. https://doi.org/10.1016/0304-3800(94)00042-G

54. Melbourne-Thomas J, Johnson C, Perez P, Eustache J, Fulton E, Cleland D. Coupling biophysical and socioeconomic models for coral reef systems in Quintana Roo, Mexican Caribbean. Ecol Soc. 2011; 16. Available: http://www.ecologyandsociety.org/vol16/iss3/art23/main.html

55. Izuka SK, Engott JA, Bassiouni M, Johnson AG, Miller LD, Rotzoll K, et al. Volcanic aquifers of Hawai'i—Hydrogeology, water budgets, and conceptual models [Internet]. Reston, VA: U.S. Geological Survey; 2016 p. 172. Report No.: 2015–5164. http://pubs.er.usgs.gov/publication/sir20155164

56. Slomp CP, Van Cappellen P. Nutrient inputs to the coastal ocean through submarine groundwater discharge: controls and potential impact. J Hydrol. 2004; 295: 64–86.

57. Moore WS. The effect of submarine groundwater discharge on the ocean. Annu Rev Mar Sci. 2010; 2: 59–88.

58. Prouty NG, Swarzenski PW, Fackrell J, Johannesson KH, Palmore CD. Groundwater-derived nutrient and trace element transport to a nearshore Kona coral ecosystem: Experimental mixing model results. J Hydrol Reg Stud. 2016; https://doi.org/10.1016/j.ejrh.2015.12.058

59. Street JH, Knee KL, Grossman EE, Paytan A. Submarine groundwater discharge and nutrient addition to the coastal zone and coral reefs of leeward Hawai'i. Mar Chem. 2008; 109: 355–376.

60. Knee KL, Street JH, Grossman EE, Boehm AB, Paytan A. Nutrient inputs to the coastal ocean from submarine groundwater discharge in a groundwater-dominated system: Relation to land use (Kona coast, Hawaii, U.S.A.). Limnol Oceanogr. 2010; 55: 1105–1122. https://doi.org/10.4319/lo.2010.55.3.1105

61. Kim G, Kim J-S, Hwang D-W. Submarine groundwater discharge from oceanic islands standing in oligotrophic oceans: Implications for global biological production and organic carbon fluxes. Limnol Oceanogr. 2011; 56: 673–682.

62. Knee KL, Layton BA, Street JH, Boehm AB, Paytan A. Sources of Nutrients and Fecal Indicator Bacteria to Nearshore Waters on the North Shore of Kaua'i (Hawai'i, USA). Estuaries Coasts. 2008; 31: 607–622. https://doi.org/10.1007/s12237-008-9055-6

63. Costa BM, Kendall M. Marine Biogeography Assessment of the Main Hawaiian Islands. Bureau of Ocean Energy Management and National Oceanic and Atmospheric Administration. OCS Study BOEM 2016–035 and NOAA Technical Memorandum NOS NCCOS 214. 359 pp.; 2016.

64. Calhoun RS, Fletcher CH. Measured and predicted sediment yield from a subtropical, heavy rainfall, steep-sided river basin: Hanalei, Kauai, Hawaiian Islands. Geomorphology. 1999; 30: 213–226. https://doi.org/10.1016/S0169-555X(99)00030-6

65. Delaney DG, Teneva LT, Stamoulis KA, Giddens JL, Koike H, Ogawa T, et al. Patterns in artisanal coral reef fisheries reveal best practices for monitoring and management [Internet]. PeerJ Preprints; 2017 Jul. Report No.: e3076v1. https://doi.org/10.7287/peerj.preprints.3076v1

66. Vitousek S, Barbee MM, Fletcher CH, Richmond BM, Genz AS. Pu'ukoholā Heiau National Historic Site and Kaloko Honokōhau Historical Park, Big Island of Hawai'i. Honolulu, HI, USA: NPS Geologic Resources Division; 2009.

67. Smith JE, Brainard R, Carter A, Grillo S, Edwards C, Harris J, et al. Re-evaluating the health of coral reef communities: baselines and evidence for human impacts across the central Pacific. Proc R Soc B. 2016; 283: 20151985. https://doi.org/10.1098/rspb.2015.1985 PMID: 26740615

68. Friedlander A, Poepoe K, Poepoe K, Helm K, Bartram P, Maragos J, et al. Application of Hawaiian traditions to community-based fishery management. Proceedings of the Ninth International Coral Reef Symposium, Bali, 23–27 October 2000, 2002. pp. 813–815. http://www.coremap.or.id/downloads/ICRS9th-Friedlander.pdf

69. Poepoe KK, Bartram PK, Friedlander AM, Haggan N, Neis B, Baird IG. The use of traditional knowledge in the contemporary management of a Hawaiian community's marine resources. Fish Knowl Fish Sci Manag. 2005; http://www.academia.edu/download/35590757/Fishers_Knowledge_2014.pdf#page=94

70. Vaughan MB, Vitousek PM. Mahele: Sustaining Communities through Small-Scale Inshore Fishery Catch and Sharing Networks. Pac Sci. 2013; 67: 329–344. https://doi.org/10.2984/67.3.3

71. Goodell W. Coupling remote sensing with in-situ surveys to determine reef fish habitat associations for the design of marine protected areas. Masters dissertation, The University of Hawai'i. 2015.

72. Minton D, Conklin E, Friedlander A, Most R, Pollock K, Stamoulis K, et al. Establishing the Baseline Condition of the Marine Resources: Results of the 2012 and 2013 Ka'ūpūlehu, Hawai'i Marine Surveys. The Nature Conservancy; 2015 pp. 1–46.

73. Pollock DW. User's guide for MODPATH/MODPATH-PLOT, Version 3; a particle tracking post-processing package for MODFLOW, the U.S. Geological Survey finite-difference ground-water flow model [Internet]. The Survey; U.S. Geological Survey, Earth Science Information Center [distributor],; 1994. Report No.: 94–464. http://pubs.er.usgs.gov/publication/ofr94464

74. Pollock DW. USGS Techniques and Methods 6-A41: User Guide for MODPATH Version 6—A Particle-Tracking Model for MODFLOW [Internet]. 2012 pp. 1–58. https://pubs.usgs.gov/tm/6a41/

75. Freeze RA, Cherry JA. Groundwater. Prentice-Hall; 1979.

76. Harbaugh AW. The U.S. Geological Survey Modular Ground-Water Model—the Ground-Water Flow Process. U.S. Department of the Interior & U.S. Geological Survey; 2005.

77. Shade PJ. Water Budget for the Island of Kauai, Hawaii [Internet]. Geological Survey (U.S.); 1995. Report No.: 95–4128. http://pubs.er.usgs.gov/publication/wri954128

78. Engott JA. A Water-Budget Model and Assessment of Groundwater Recharge for the Island of Hawai'i [Internet]. 2011 pp. 1–53. Report No.: 2011–5078. https://pubs.usgs.gov/sir/2011/5078/

79. State of Hawaii. Data for Underground Injection Control Permit Number UH-1927, Flow and Chemistry Data. Hawaii Dept. of Health, Safe Drinking Water Branch; 2003.

80. USGS. USGS 16108000 Wainiha River nr Hanalei, Kauai, HI. In: USGS National Water Information System: Web Interface [Internet]. 2017. https://nwis.waterdata.usgs.gov/nwis/inventory/?site_no=16108000&agency_cd=USGS

81. White KE, Sloto RA. Base-flow frequency characteristics of selected Pennsylvania streams [Internet]. U.S. Geological Survey ; Books and Open-File Reports Section [distributor],; 1990. Report No.: 90–4160. http://pubs.er.usgs.gov/publication/wri904160

82. State of Hawaii. Groundwater pumping records for Hawaii Island. State of Hawaii Commission on Water Resources Management; 2015.

83. Zheng C, Wang PP. MT3DMS: A modular three-dimensional multi-species transport model for simulation of advection, dispersion and chemical reactions of contaminants in groundwater systems; documentation and user's guide [Internet]. Vicksburg, Mississippi, USA: U.S. Army Engineer Research and Development Center; 1999. Report No.: Report SERDP-99-1. https://cfpub.epa.gov/si/si_public_record_Report.cfm?dirEntryID=19970

84. Marion GM. The Geochemistry of Natural Waters: Surface and Groundwater Environments. J Environ Qual. 1998; 27: 245.

85. Wiedemeier TH. Natural attenuation of fuels and chlorinated solvents in the subsurface [Internet]. John Wiley & Sons; 1999. https://books.google.com/books?hl=en&lr=&id=LVYRrozBhqcC&oi=fnd&pg=PR11&dq=Natural+attenuation+of+fuels+and+chlorinated+solvents+in+the+subsurface&ots=NztD1rTo-P&sig=Wkiup8yyqkoM9y1ziSo9328nDBI

86. Soldat DJ, Petrovic AM. The Fate and Transport of Phosphorus in Turfgrass Ecosystems. Crop Sci. 2008; 48: 2051–2065. https://doi.org/10.2135/cropsci2008.03.0134

87. Potter SR, Andrews S, Atwood JD, Kellog RL, Lemunyon J, Norfleet L, et al. Model Simulation of Soil Loss, Nutrient Loss, and Change in Soil Organic Caron Associated with Crop Production [Internet]. 2006 p. 262. https://www.nrcs.usda.gov/Internet/FSE_DOCUMENTS/nrcs143_013138.pdf

88. Glenn CR, Whittier RB, Dailer ML, Dulaiova H, El-Kadi AI, Fackrell J, et al. Lahaina Groundwater Tracer Study–Lahaina, Maui, Hawaii. 2013; https://works.bepress.com/jacque_kelly/4/

89. Bienfang P. Water Quality Characteristics of Honokohau Harbor: A Subtropical Embayment Affected by Groundwater Intrusion. 1980; http://scholarspace.manoa.hawaii.edu/handle/10125/1627

90. State of Hawaii. Drinking Water Contaminant Database, nitrate data for Kauai. Hawaii Dept. of Health, Safe Drinking Water Branch; 2016.

91. Fackrell J. Geochemical Evolution of Hawaiian Groundwater. Natural and Anthropogenic Controls on Groundwater Nutrient and Dissolved Inorganic Carbon Concentrations; West Hawai'i, USA. Phd Dissertation. University of Hawai'i, Dept. of Geology and Geophysics; 2016. pp. 68–99.

92. U.S. EPA. Onsite Wastewater Treatment Systems Manual [Internet]. 2002 pp. 1–367. http://www.epa.gov/ORD/NRMRL/Pubs/625180012/625180012.htm

93. Whittier RB, El-Kadi A. Human health and environmental risk ranking of on-site sewage disposal systems for the Hawaiian Islands of Kauai, Molokai, Maui, and Hawaii. Final Rep Prep State Hawaii Dep Health Safe Drink Water Branch. 2014; http://health.hawaii.gov/wastewater/files/2015/09/OSDS_NI.pdf

94. HDOH. Work Plan and Sampling and Analysis Plan for Upcountry Maui Groundwater Nitrate Investigation. Honolulu, HI, USA: Hawaii Department of Health; 2017.

95. Lowe KS, Tucholke MB, Tomaras JM, Conn K, Hoppe C, Drewes JE, et al. Influent constituent characteristics of the modern waste stream from single sources. Water Environ Res Found. 2009; 202.

96. Tasato GT, Dugan GL. WRRCTR No.131 Leachate Quality from Lysimeters Treating Domestic Sewage [Internet]. Water Resources Research Center, University of Hawaii at Manoa; 1980 Apr. http://scholarspace.manoa.hawaii.edu/handle/10125/2265

97. Wang W, Haver D, Pataki DE. Nitrogen budgets of urban lawns under three different management regimes in southern California. Biogeochemistry. 2014; 121: 127–148.

98. Throssell CS, Lyman GT, Johnson ME, Stacey GA, Brown CD. Golf course environmental profile measures nutrient use and management and fertilizer restrictions, storage, and equipment calibration. Appl Turfgrass Sci. 2009; 6: 0–0.

99. CH2MHill. Hawaii Water Conservation Plan–Final Report. Honolulu, Hawaii, USA; 2003 p. 324.

100. Falinski KA. Predicting sediment export into tropical coastal ecosystems to Support ridge to reef management [Internet]. Honolulu, Hawaii, USA: University of Hawaii at Manoa; 2016 May pp. 1–304. https://search.proquest.com/openview/5cb8784b884e008058d6c0fa9226b27f/1.pdf?pq-origsite=gscholar&cbl=18750&diss=y

101. Xiaobin Z. Groundwater modeling system (GMS) software. Hydrogeol Eng Geol. 2003; 5: 53–55.

102. Oki T, Nishimura T, Dirmeyer P. Assessment of Annual Runoff from Land Surface Models Using Total Runoff Integrating Pathways (TRIP). J Meteorol Soc Jpn Ser II. 1999; 77: 235–255.

103. Amato DW, Bishop JM, Glenn CR, Dulai H, Smith CM. Impact of Submarine Groundwater Discharge on Marine Water Quality and Reef Biota of Maui. PLOS ONE. 2016; 11: e0165825. https://doi.org/10.1371/journal.pone.0165825 PMID: 27812171

104. Harbaugh AW. A computer program for calculating subregional water budgets using results from the U.S. Geological Survey Modular Three-Dimensional Finite- Difference Ground-Water Flow Model [Internet]. U.S. Geological Survey; Books and Open-File Reports Section [distributor],; 1990. Report No.: 90–392. http://pubs.er.usgs.gov/publication/ofr90392

105. Yu C, Lee JAY, Munro-Stasiuk MJ. Extensions to least-cost path algorithms for roadway planning. Int J Geogr Inf Sci. 2003; 17: 361–376.

106. Derse E, Knee KL, Wankel SD, Kendall C, Berg Carl J, Paytan A. Identifying Sources of Nitrogen to Hanalei Bay, Kauai, Utilizing the Nitrogen Isotope Signature of Macroalgae. Environ Sci Technol. 2007; 41: 5217–5223. https://doi.org/10.1021/es0700449 PMID: 17822082

107. Garrison GH, Glenn CR, McMurtry GM. Measurement of submarine groundwater discharge in Kahana Bay, O'ahu, Hawai'i. Limnol Oceanogr. 2003; 48: 920–928. https://doi.org/10.4319/lo.2003.48.2.0920

108. Paytan A, Shellenbarger GG, Street JH, Gonneea ME, Davis K, Young MB, et al. Submarine groundwater discharge: An important source of new inorganic nitrogen to coral reef ecosystems. Limnol Oceanogr. 2006; 51. https://doi.org/10.4319/lo.2006.51.1.0343

109. Fackrell JK, Glenn CR, Popp BN, Whittier RB, Dulai H. Wastewater injection, aquifer biogeochemical reactions, and resultant groundwater N fluxes to coastal waters: Kā'anapali, Maui, Hawai'i. Mar Pollut Bull. 2016; 110: 281–292. https://doi.org/10.1016/j.marpolbul.2016.06.050 PMID: 27339740

110. Stamoulis KA, Delevaux JMS, Williams ID, Poti M, Costa B, Kendall MS, et al. Seascape models reveal places to focus coastal fisheries management. Ecol Appl. accepted; https://doi.org/10.1002/eap.1696 PMID: 29421847

111. Stopa JE, Filipot J-F, Li N, Cheung KF, Chen Y-L, Vega L. Wave energy resources along the Hawaiian Island chain. Renew Energy. 2013; 55: 305–321. https://doi.org/10.1016/j.renene.2012.12.030

112. OP. Coastlines for the main hawaiian islands [Internet]. Honolulu, Hawaii, USA: Hawaii Office of Planning; 2000. http://planning.hawaii.gov/gis/download-gis-data/

113. HMRG. Bathymetry [Internet]. University of Hawai'i at Manoa, HI, USA: Hawai'i Mapping Research Group, School of Ocean and Earth Science and Technology; 2015. http://www.soest.hawaii.edu/HMRG/cms/

114. Pittman SJ, Brown KA. Multi-Scale Approach for Predicting Fish Species Distributions across Coral Reef Seascapes. PLOS ONE. 2011; 6: e20583. https://doi.org/10.1371/journal.pone.0020583 PMID: 21637787

115. Kendall MS, Miller TJ, Pittman SJ. Patterns of scale-dependency and the influence of map resolution on the seascape ecology of reef fish. Mar Ecol Prog Ser. 2011; 427: 259–274.

116. Legendre P, Anderson MJ. Distance-Based Redundancy Analysis: Testing Multispecies Responses in Multifactorial Ecological Experiments. Ecol Monogr. 1999; 69: 1–24. https://doi.org/10.1890/0012-9615(1999)069[0001:DBRATM]2.0.CO;2

117. McArdle BH, Anderson MJ. Fitting Multivariate Models to Community Data: A Comment on Distance-Based Redundancy Analysis. Ecology. 2001; 82: 290–297. https://doi.org/10.1890/0012-9658(2001)082[0290:FMMTCD]2.0.CO;2

118. Stamoulis KA, Friedlander AM. A seascape approach to investigating fish spillover across a marine protected area boundary in Hawai'i. Fish Res. 2013; 144: 2–14. https://doi.org/10.1016/j.fishres.2012.09.016

119. Franklin J. Mapping Species Distributions: Spatial Inference and Prediction. Cambridge University Press; 2010.

120. Breiman L. Bagging predictors. Mach Learn. 1996; 24: 123–140. https://doi.org/10.1007/BF00058655

121. Breiman L. Statistical Modeling: The Two Cultures (with comments and a rejoinder by the author). Stat Sci. 2001; 16: 199–231. https://doi.org/10.1214/ss/1009213726

122. De'ath G, Fabricius KE. Classification and Regression Trees: A Powerful yet Simple Technique for Ecological Data Analysis. Ecology. 2000; 81: 3178–3192. https://doi.org/10.1890/0012-9658(2000)081[3178:CARTAP]2.0.CO;2

123. Elith J, Leathwick JR, Hastie T. A working guide to boosted regression trees. J Anim Ecol. 2008; 77: 802–813. https://doi.org/10.1111/j.1365-2656.2008.01390.x PMID: 18397250

124. Venables WN, Ripley BD. Modern Applied Statistics with S-PLUS. Springer Science & Business Media; 2013.

125. Ridgeway G. Generalized Boosted Models: A guide to the gbm package. 2007.

126. R Core Team. R: A language and environment for statistical computing [Internet]. Vienna, Austria.: R Foundation for Statistical Computing; 2014. http://www.r-project.org

127. Miller JA. Species distribution models: Spatial autocorrelation and non-stationarity. Prog Phys Geogr. 2012; 36: 681–692. https://doi.org/10.1177/0309133312442522

128. Hijmans RJ. R package, Raster: Geographic data analysis and modeling. Software [Internet]. 2014. http://CRAN.R-project.org/package=raster

129. Hijmans RJ, Phillips S, Leathwick J, Elith J. R package, dismo: Species distribution modeling [Internet]. 2014. http://CRAN.R-project.org/package=dismo

130. Friedlander AM, Parrish JD. Habitat characteristics affecting fish assemblages on a Hawaiian coral reef. J Exp Mar Biol Ecol. 1998; 224: 1–30. https://doi.org/10.1016/S0022-0981(97)00164-0

131. Grigg RW. Holocene coral reef accretion in Hawaii: a function of wave exposure and sea level history. Coral Reefs. 1998; 17: 263–272. https://doi.org/10.1007/s003380050127

132. Engels MS, Fletcher CH, Field ME, Storlazzi CD, Grossman EE, Rooney JJ, et al. Holocene reef accretion: southwest Molokai, Hawaii, USA. J Sediment Res. 2004; 74: 255–269.

133. De'ath G, Fabricius K. Water quality as a regional driver of coral biodiversity and macroalgae on the Great Barrier Reef. Ecol Appl. 2010; 20: 840–850. https://doi.org/10.1890/08-2023.1 PMID: 20437968

134. Vermeij MJA, van Moorselaar I, Engelhard S, Hörnlein C, Vonk SM, Visser PM. The Effects of Nutrient Enrichment and Herbivore Abundance on the Ability of Turf Algae to Overgrow Coral in the Caribbean. PLOS ONE. 2010; 5: e14312. https://doi.org/10.1371/journal.pone.0014312 PMID: 21179215

135. Bruce T, Meirelles PM, Garcia G, Paranhos R, Rezende CE, de Moura RL, et al. Abrolhos Bank Reef Health Evaluated by Means of Water Quality, Microbial Diversity, Benthic Cover, and Fish Biomass Data. PLOS ONE. 2012; 7: e36687. https://doi.org/10.1371/journal.pone.0036687 PMID: 22679480

136. Johnson AG, Glenn CR, Burnett WC, Peterson RN, Lucey PG. Aerial infrared imaging reveals large nutrient-rich groundwater inputs to the ocean. Geophys Res Lett. 2008; 35. Available: http://onlinelibrary.wiley.com/doi/10.1029/2008GL034574/full

137. Selvarajah N, Maggs GR, Crush JR, Ledgard SF. Nitrate in ground water in the Waikato region. The Efficient Use of Fertilisers in a Changing Environment: reconciling productivity with sustainability Proceedings of the 7 th Annual Workshop (Feb, 1994) Fertiliser and Lime Research Centre, Massey University, Palmerston North. 1994. https://www.researchgate.net/profile/Selva_Selvarajah/publication/269337826_NITRATE_IN_GROUND_WATER_IN_THE_WAIKATO_REGION/links/54879db50cf289302e2edde4.pdf

138. Fackrell J, Glenn CR, Thomas D, Whittier R, Popp B. Development and Hydrogeologic Application of a Local Meteoric Water Line for West Hawai'i, USA. Journal of Hydrology: Regional Studies. J Hydrol Reg Stud. in press;

139. Hwang D, Lee Y-W, Kim G. Large submarine groundwater discharge and benthic eutrophication in Bangdu Bay on volcanic Jeju Island, Korea. Limnol Oceanogr. 2005; 50: 1393–1403.

140. Bokuniewicz H, Coffey R, Charette MA. Character of submarine groundwater discharge around islands. AGU Fall Meeting Abstracts. 2009. p. 03. http://adsabs.harvard.edu/abs/2009AGUFM.H13H..03B

141. Smith SV, Kimmerer WJ, Laws EA, Brock RE, Walsh TW. Kaneohe Bay sewage diversion experiment: perspectives on ecosystem responses to nutritional perturbation. Pac Sci. 1981; 35: 279–395.

142. Walker DI, Ormond RFG. Coral death from sewage and phosphate pollution at Aqaba, Red Sea. Mar Pollut Bull. 1982; 13: 21–25. https://doi.org/10.1016/0025-326X(82)90492-1

143. Lapointe BE, Barile PJ, Littler MM, Littler DS. Macroalgal blooms on southeast Florida coral reefs: II. Cross-shelf discrimination of nitrogen sources indicates widespread assimilation of sewage nitrogen. Harmful Algae. 2005; 4: 1106–1122. https://doi.org/10.1016/j.hal.2005.06.002

144. Bell PRF. Eutrophication and coral reefs—some examples in the Great Barrier Reef lagoon. Water Res. 1992; 26: 553–568. https://doi.org/10.1016/0043-1354(92)90228-V

145. Whittier RB, El-Kadi AI. Human and Environmental Risk Ranking of Onsite Sewage Disposal Systems: Molokai, Maui, and Hawai'i. Honolulu, Hawai'i: State of Hawai'i Department of Health, Safe Drinking Water Branch; 2014 pp. 1–258.

146. Dollar SJ, Atkinson M, Atkinson S. Investigation the relationship between cesspool nutrients and abundance of Hypnea musciformis in West Maui, Hawaii. Honolulu, Hawaii.: Report State of Hawaii Department of Health; 1999.

147. Dollar SJ, Atkinson MJ. Effects of nutrient subsidies from groundwater to nearshore marine ecosystems off the island of Hawaii. Estuar Coast Shelf Sci. 1992; 35: 409–424. https://doi.org/10.1016/S0272-7714(05)80036-8

148. Adey WH. Coralline algae as indicators of sea-level. In: van de Plassche O, editor. Sea-Level Research. Springer Netherlands; 1986. pp. 229–280. https://doi.org/10.1007/978-94-009-4215-8_9

149. Bahr KD, Jokiel PL, Toonen RJ. The unnatural history of Kāne'ohe Bay: coral reef resilience in the face of centuries of anthropogenic impacts. PeerJ. 2015; 3: e950. https://doi.org/10.7717/peerj.950 PMID: 26020007

150. Duarte TK, Pongkijvorasin S, Roumasset J, Amato D, Burnett K. Optimal management of a Hawaiian Coastal aquifer with nearshore marine ecological interactions. Water Resour Res. 2010; 46: W11545. https://doi.org/10.1029/2010WR009094

151. Wu NY., Chung KC. Tolerance of Pomacanthus imperator to hypoosmotic salinities: changes in body composition and hepatic enzyme activities. J Fish Biol. 1995; 47: 70–81.

152. Smith JE, Shaw M, Edwards RA, Obura D, Pantos O, Sala E, et al. Indirect effects of algae on coral: algae-mediated, microbe-induced coral mortality. Ecol Lett. 2006; 9: 835–845. https://doi.org/10.1111/j.1461-0248.2006.00937.x PMID: 16796574

153. Fletcher CH, Bochicchio C, Conger CL, Engels MS, Feirstein EJ, Frazer N, et al. Geology of Hawaii Reefs. In: Riegl BM, Dodge RE, editors. Coral Reefs of the USA. Springer Netherlands; 2008. pp. 435–487. https://doi.org/10.1007/978-1-4020-6847-8_11

154. Jokiel PL, Brown EK, Friedlander A, Rodgers SK, Smith WR. Hawai'i Coral Reef Assessment and Monitoring Program: Spatial Patterns and Temporal Dynamics in Reef Coral Communities. Pac Sci. 2004; 58: 159–174. https://doi.org/10.1353/psc.2004.0018

155. Friedlander A, Goodel W, Stamoulis KA. Ecological Assessment of Hā'ena reef habitats. Fisheries Ecology Research Lab, University of Hawai'i at Mānoa; 2014 pp. 1–16.

156. Friedlander AM, Parrish JD. Temporal dynamics of fish communities on an exposed shoreline in Hawaii. Environ Biol Fishes. 1998; 53: 1–18. https://doi.org/10.1023/A:1007497210998

157. DeMartini EE, Parrish FA, Parrish JD. Interdecadal Change in Reef Fish Populations at French Frigate Shoals and Midway Atoll, Northwestern Hawaiian Islands: Statistical Power in Retrospect. Bull Mar Sci. 1996; 58: 804–825.

158. Friedlander AM, Brown EK, Jokiel PL, Smith WR, Rodgers KS. Effects of habitat, wave exposure, and marine protected area status on coral reef fish assemblages in the Hawaiian archipelago. Coral Reefs. 2003; 22: 291–305. https://doi.org/10.1007/s00338-003-0317-2

159. Stamoulis KA, Poti M, Delevaux JMS, Donovan MK, Friedlander A, Kendall MS. Chapter 4: Fishes—Reef Fish. Marine Biogeographic Assessment of the Main Hawaiian Islands. B.M. Costa and M.S. Kendall. Bureau of Ocean Energy Management and National Oceanic and Atmospheric Administration. OCS Study BOEM 2016–035 and NOAA Technical Memorandum NOS NCCOS 214. 359 pp.; 2016. pp. 156–196.

160. Goetze JS, Langlois TJ, Egli DP, Harvey ES. Evidence of artisanal fishing impacts and depth refuge in assemblages of Fijian reef fish. Coral Reefs. 2011; 30: 507–517.

161. Jokiel PL. Effects of water motion on reef corals. J Exp Mar Biol Ecol. 1978; 35: 87–97. https://doi.org/10.1016/0022-0981(78)90092-8

162. Friedlander AM, Brown EK. Hanalei bay, Kaua'i marine benthic communities since 1992: spatial and temporal trends in a dynamic Hawaiian coral reef ecosystem. Pacific Island Ecosystems Research Center of the U.S. Geological Survey; 2006 pp. 1–44.

163. Bellwood DR, Hughes TP, Folke C, Nyström M. Confronting the coral reef crisis. Nature. 2004; 429: 827–833. https://doi.org/10.1038/nature02691 PMID: 15215854

164. DAR. Management Plan for the Hā'ena Community-Based Subsistence Fisheries Area, Kauai [Internet]. Hawaii Department of Land and Natural Resources: Division of Aquatic Resources; 2016. https://dlnr.hawaii.gov/dar/files/2016/08/Haena_CBSFA_Mgmt_Plan_8.2016.pdf

165. TNC. Ka'ūpūlehu Conservation Action Plan. The Nature Conservancy; 2015.

166. Pittman SJ, Costa BM, Battista TA. Using Lidar Bathymetry and Boosted Regression Trees to Predict the Diversity and Abundance of Fish and Corals. J Coast Res. 2009; 27–38. https://doi.org/10.2112/SI53-004.1

167. Stamoulis KA, Delevaux JMS. Data requirements and tools to operationalize marine spatial planning in the United States. Ocean Coast Manag. 2015; 116: 214–223. https://doi.org/10.1016/j.ocecoaman.2015.07.011

168. Melbourne-Thomas J, Johnson CR, Fung T, Seymour RM, Chérubin LM, Arias-González JE, et al. Regional-scale scenario modeling for coral reefs: a decision support tool to inform management of a complex system. Ecol Appl. 2011; 21: 1380–1398. https://doi.org/10.1890/09-1564.1 PMID: 21774437

169. Carlson KM, Wiegner TN. Effects of submarine groundwater discharge on bacterial growth efficiency in coastal Hawaiian waters. Aquat Microb Ecol. 2016; 77: 167–181.